

blood

2010 116: 4631-4638
Prepublished online Aug 20, 2010;
doi:10.1182/blood-2010-05-282426

Down syndrome and GATA1 mutations in transient abnormal myeloproliferative disorder: mutation classes correlate with progression to myeloid leukemia

Rika Kanezaki, Tsutomu Toki, Kiminori Terui, Gang Xu, RuNan Wang, Akira Shimada, Asahito Hama, Hirokazu Kanegane, Kiyoshi Kawakami, Mikiya Endo, Daisuke Hasegawa, Kazuhiro Kogawa, Souichi Adachi, Yasuhiko Ikeda, Shotaro Iwamoto, Takashi Taga, Yoshiyuki Kosaka, Seiji Kojima, Yasuhide Hayashi and Etsuro Ito

Updated information and services can be found at:

<http://bloodjournal.hematologylibrary.org/cgi/content/full/116/22/4631>

Articles on similar topics may be found in the following *Blood* collections:

Myeloid Neoplasia (360 articles)

Information about reproducing this article in parts or in its entirety may be found online at:

http://bloodjournal.hematologylibrary.org/misc/rights.dtl#repub_requests

Information about ordering reprints may be found online at:

<http://bloodjournal.hematologylibrary.org/misc/rights.dtl#reprints>

Information about subscriptions and ASH membership may be found online at:

<http://bloodjournal.hematologylibrary.org/subscriptions/index.dtl>

Blood (print ISSN 0006-4971, online ISSN 1528-0020), is published semimonthly by the American Society of Hematology, 1900 M St, NW, Suite 200, Washington DC 20036.

Copyright 2007 by The American Society of Hematology; all rights reserved.



Down syndrome and *GATA1* mutations in transient abnormal myeloproliferative disorder: mutation classes correlate with progression to myeloid leukemia

*Rika Kanezaki,¹ *Tsutomu Toki,¹ Kiminori Terui,¹ Gang Xu,¹ RuNan Wang,¹ Akira Shimada,² Asahito Hama,³ Hirokazu Kanegane,⁴ Kiyoshi Kawakami,⁵ Mikiya Endo,⁶ Daisuke Hasegawa,⁷ Kazuhiro Kogawa,⁸ Souichi Adachi,⁹ Yasuhiko Ikeda,¹⁰ Shotaro Iwamoto,¹¹ Takashi Taga,¹² Yoshiyuki Kosaka,¹³ Seiji Kojima,³ Yasuhide Hayashi,² and Etsuro Ito¹

¹Department of Pediatrics, Hirosaki University Graduate School of Medicine, Hirosaki, Japan; ²Department of Hematology/Oncology, Gunma Children's Medical Center, Gunma, Japan; ³Department of Pediatrics, Nagoya University Graduate School of Medicine, Nagoya, Japan; ⁴Department of Pediatrics, Graduate School of Medicine, University of Toyama, Toyama, Japan; ⁵Department of Pediatrics, Kagoshima City Hospital, Kagoshima, Japan; ⁶Department of Pediatrics, Iwate Medical University, Morioka, Japan; ⁷Department of Pediatrics, St Luke's International Hospital, Tokyo, Japan; ⁸Department of Pediatrics, National Defense Medical College, Tokorozawa, Japan; ⁹Department of Pediatrics, Kyoto University Graduate School of Medicine, Kyoto, Japan; ¹⁰Department of Pediatrics, Aomori City Hospital, Aomori, Japan; ¹¹Department of Pediatrics, Mie University Graduate School of Medicine, Tsu, Japan; ¹²Department of Pediatrics, Shiga University of Medical Science, Ohtsu, Japan; and ¹³Department of Hematology and Oncology, Hyogo Children Hospital, Kobe, Japan

Twenty percent to 30% of transient abnormal myelopoiesis (TAM) observed in newborns with Down syndrome (DS) develop myeloid leukemia of DS (ML-DS). Most cases of TAM carry somatic *GATA1* mutations resulting in the exclusive expression of a truncated protein (GATA1s). However, there are no reports on the expression levels of GATA1s in TAM blasts, and the risk factors for the progression to ML-DS are unidentified. To test whether the spectrum of transcripts

derived from the mutant *GATA1* genes affects the expression levels, we classified the mutations according to the types of transcripts, and investigated the modalities of expression by in vitro transfection experiments using *GATA1* expression constructs harboring mutations. We show here that the mutations affected the amount of mutant protein. Based on our estimates of GATA1s protein expression, the mutations were classified into GATA1s high and low groups. Phenotypic analy-

ses of 66 TAM patients with *GATA1* mutations revealed that GATA1s low mutations were significantly associated with a risk of progression to ML-DS ($P < .001$) and lower white blood cell counts ($P = .004$). Our study indicates that quantitative differences in mutant protein levels have significant effects on the phenotype of TAM and warrants further investigation in a prospective study. (*Blood*. 2010;116(22):4631-4638)

Introduction

In children with Down syndrome (DS), the risk of developing acute megakaryocytic leukemia (AMKL) is estimated at 500 times higher than in children without DS. Interestingly, neonates with DS are at a high risk of developing a hematologic disorder referred to as transient abnormal myelopoiesis (TAM). It has been estimated that 5% to 10% of infants with DS exhibit the disorder, and in most cases, it resolves spontaneously within 3 months. However, approximately 20% of the severe cases are still subject to fatal complications and 20% to 30% of patients who escape from early death develop AMKL referred to as myeloid leukemia of DS (ML-DS) within 4 years.¹⁻⁴

Recent studies found that high white blood cell (WBC) count, failure of spontaneous remission, early gestational age (EGA) and liver fibrosis or liver dysfunction are significantly associated with early death.⁵⁻⁷ Most of the same covariates were found in all of the reports. However, the risk factors for the progression to ML-DS remain elusive.

Blast cells in most patients with TAM and ML-DS have mutations in exon 2 of the gene coding the transcription factor *GATA1*,⁸⁻¹⁴ which is essential for normal development of erythroid and megakaryocytic cells.¹⁵⁻¹⁸ The mutations lead to exclusive expression of a truncated *GATA1* protein (referred to as GATA1s)

translated from the second methionine on exon 3. These findings strongly suggest that the qualitative deficit of *GATA1* contributes to the genesis of TAM and ML-DS. The analysis of megakaryocyte-specific knockdown of *GATA1* in vivo has revealed a critical role for this factor in megakaryocytic development. Reduced expression (or complete absence) of *GATA1* in megakaryocytes leads to increased proliferation and deficient maturation as well as a reduced number of circulating platelets.^{19,20} Mice harboring a heterozygous *GATA1* knockdown allele frequently develop erythroblastic leukemia.²¹ These observations indicate that the expression levels of *GATA1* are crucial for the proper development of erythroid and megakaryocytic cells and compromised *GATA1* expression is a causal factor in leukemia.²² Nevertheless, the impact of a quantitative deficit of the factor on the pathogenesis of TAM and ML-DS has not been examined.

In this study, we classified the *GATA1* mutations observed in TAM patients according to the types of transcripts, and investigated the modalities of gene expression by in vitro transfection assays using *GATA1* expression constructs. We report here that the spectrum of the transcripts derived from the mutant genes affects protein expression and the risk of progression from TAM to ML-DS.

Submitted April 30, 2010; accepted August 2, 2010. Prepublished online as *Blood* First Edition paper, August 20, 2010; DOI 10.1182/blood-2010-05-282426.

*R.K. and T.T. contributed equally to this work.

The online version of this article contains a data supplement.

The publication costs of this article were defrayed in part by page charge payment. Therefore, and solely to indicate this fact, this article is hereby marked "advertisement" in accordance with 18 USC section 1734.

© 2010 by The American Society of Hematology

Methods

Patients

This study was approved by the Ethics Committee of Hirosaki University Graduate School of Medicine, and all clinical samples were obtained with informed consent from the parents of all patients with TAM, in accordance with the Declaration of Helsinki. The following clinical data were collected: sex, gestational age, birth weight, time of diagnosis, symptom at diagnosis, and clinical presentation. The following laboratory data were obtained: a complete blood cell count at diagnosis including WBC and the percentage of blasts in the peripheral blood, coagulation parameters, liver enzymes (alanine aminotransferase and aspartate aminotransferase), and total bilirubin. The procedure for the detection of *GATA1* mutations was described previously.¹³ Genomic DNA was directly extracted from peripheral blood or bone marrow with the QIAamp blood mini kit (QIAGEN). Total RNA was extracted from white blood cells prepared by removal of erythrocytes by hypotonic buffer treatment of peripheral blood. Clinical features, outcomes, and characteristics of *GATA1* mutations are indicated in Table 1.

Construction of *GATA1* expression vectors

To construct *GATA1* minigene expression vectors, fragments of the normal human *GATA1* gene from a part of intron 1 to the stop codon located on exon 6 were amplified by polymerase chain reaction (PCR; Prime STAR HS; Takara Bio) and subcloned to mammalian expression vector pcDNA3.1 (+)/Neo (Invitrogen). To introduce mutations identical to those observed in TAM patients into the expression vector, the regions containing mutations were amplified by PCR from patient samples and inserted into the expression plasmid. To construct expression vectors carrying cDNA, we performed PCR using cDNA derived from baby hamster kidney 21 (BHK-21) cells transfected with *GATA1* minigene vectors. The PCR products were subcloned to pcDNA3.1(+)/Neo. Details of the sequence of each expression construct are described in Table 2.

Transfection

BHK-21, a baby hamster kidney fibroblast cell line, was cultured with Dulbecco modified Eagle medium supplemented 10% fetal bovine serum. *GATA1* expression vectors were transfected into BHK-21 cells using FuGENE HD transfection reagent (Roche Diagnostics) according to the manufacturer's methods. After 24 hours, protein and total RNA were extracted.

Western blot analysis

Lysates of transfected BHK-21 cells were transferred to Hybond-P (GE Healthcare) and processed for reaction with anti-*GATA1* antibody M-20 (Santa Cruz Biotechnology) or anti-neomycin phosphotransferase II (NeoR) antibody (Millipore) as described previously.²³

Northern blot analysis

Two micrograms of total RNA were transferred to Hybond-N+ (GE Healthcare) and hybridized with *GATA1* or *NeoR* DNA probe. Hybridization and detection were performed with the Gene Images AlkPhos Direct Labeling and Detection System (GE Healthcare) according to the manufacturer's instructions.

RT-PCR

To detect alternatively spliced transcripts derived from *GATA1* minigene constructs or from patients' peripheral blood mononuclear cells (obtained by Ficoll-Hypaque fractionation), we performed reverse transcription (RT)-PCR using primers T7: 5' AATACGACTCACTATAG 3' and *GATA1* AS1, and *GATA1* S1 and *GATA1* AS1, respectively.¹³ Densitometric analyses were performed by the Quantity-One software (Version 4.5.2; Bio-Rad Laboratories).

Statistical analysis

The cumulative incidence of the progression to ML-DS was analyzed with the Gray test. Differences in the distribution of individual parameters among patient subsets were analyzed using the Pearson χ^2 test or Fisher exact test for categorized variables and the Mann-Whitney *U* test for continuous variables. The univariate Cox proportional hazards model was used to obtain the estimates and the 95% confidence interval of the relative risk for prognostic factors.

Results

Patient characteristics and outcomes

From 2003 to 2008, we screened *GATA1* mutations in clinical samples obtained from 78 patients with TAM upon request from referring hospitals. Acquired *GATA1* mutations were detected in a total of 72 (92.3%) patients among them. Of the 72 patients, 6 harbored multiple *GATA1* mutant clones and were excluded from this study because we could not determine a dominant clone in these patients. Those 6 have not progressed to ML-DS. For the remaining 66 patients (32 male and 34 female), the clinical characteristics and laboratory data at diagnosis are described in Table 1 and summarized in Table 3. Early death within the first 6 months of life occurred in 16 patients (24.2%). The covariates correlated with early death were as follows: EGA, low birth weight, high WBC count at diagnosis, high percentage of peripheral blast cells, complication of effusions, and bleeding diatheses. These prognostic factors were identified in previous studies.⁵⁻⁷ Eleven (16.7%) cases subsequently developed ML-DS. The median age at diagnosis of ML-DS was 396 days (range 221-747 days). Univariate analysis revealed no covariates correlated with progression to ML-DS except the low total bilirubin level at diagnosis ($P = .023$).

GATA1 mutations affect expression levels of *GATA1*s protein

We first asked whether the spectrum of transcripts derived from the mutant *GATA1* genes affected the expression levels of the translation products. The transcripts coding *GATA1*s protein were categorized into 3 groups as follows: loss of the first methionine, splicing errors, and premature termination codon (PTC). Furthermore, the PTC group was divided into 2 subcategories by the location of introduced PTC. In this report, we refer to the mutation that causes PTC before the second methionine at codon 84 as PTC type 1, and after codon 84 as PTC type 2. We constructed cDNA expression vectors for each class of mutations observed in TAM patients, and transfected these constructs into BHK-21 cells (Figure 1). The details of the *GATA1* mutations are described in Table 2. Western blot analysis revealed that *GATA1*s proteins were most abundantly expressed in mutants with splicing errors. The transcripts from mutants that had lost the first methionine were also efficiently translated. In contrast, in the cells expressing PTC type 1 or type 2 constructs, *GATA1*s expression levels were uniformly low. Note that the translation efficiency of the PTC type 2 transcripts was lowest among them.

To test the possibility that mutations in *GATA1* have an effect on the quantity of the transcripts, we next prepared human *GATA1* minigene expression vectors, and assessed the expression levels. Consistent with the results using cDNA expression vectors, Western blot analysis showed that the expression levels of *GATA1*s were lower in cells expressing PTC type 2 mutations, whereas the expression levels of the proteins from PTC type 1 mutations were not uniformly low (Figure 2Ai). Northern blot analysis revealed that the lowest expression levels of *GATA1* mRNAs were observed

Table 1. Clinical features and mutation characteristics in TAM patients with GATA1 mutations

Patient No.	Sex	WBC, $\times 10^9/L$	Outcome	GATA1 mutation*	Consequence of mutation	Mutation type
1 ^{19,24}	F	63.9	CR	207 C>G	Tyr69stop	PTC 1-3'
2 ¹⁹	F	89.0	Early death	199 G>T	Glu67stop	PTC 1-3'
3 ¹⁹	F	NA	NA	174 ins 19 bp CAGCCACCGCTGCAGCTGC	Frame shift at codon58, stop at codon 73	PTC 1-3'
4 ¹⁹	F	128.8	CR	IVS1 to IVS2 del 1415 bp	Splice mutant	Splicing error
5 ¹⁹	F	NA	NA	49 C>T	Gln17stop	PTC 1-5'
6 ¹⁹	F	248.6	NA	Loss of 2nd exon	Splice mutant	Splicing error
7 ¹⁹	F	31.2	CR	Loss of 2nd exon	Splice mutant	Splicing error
8 ¹⁹	M	199.6	CR	-11 to +33 del 44 bp	No translation from Met1	Loss of 1st Met
9 ¹⁹	M	44.9	Early death	45 ins C	Frame shift at codon15, stop at codon 39	PTC 1-5'
10 ¹⁹	M	50.9	CR	37 G>T	Glu13stop	PTC 1-5'
11 ¹⁹	F	103.0	Early death	90-91 del AG	Frame shift at codon 30, stop at codon 38	PTC 1-5'
12 ¹⁹	F	14.6	Evolved to ML-DS	116 del A	Frame shift at codon 39, stop at codon 136	PTC 2
13 ¹⁹	M	423.0	CR	185 ins 22 bp GCTGCAGCTGCGGCACCTGGCCT	Frame shift at codon 62, stop at codon 74	PTC 1-3'
14 ¹⁹	M	201.2	CR	189 C>A	Tyr63stop	PTC 1-3'
15 ¹⁹	M	NA	NA	1 A>G	No translation from Met1	Loss of 1st Met
16 ¹⁹	F	28.3	CR	189 C>A	Tyr63stop	PTC 1-3'
17 ¹⁹	M	203.0	Evolved to ML-DS	38-39 del AG	Frame shift at codon 13, stop at codon 38	PTC 1-5'
18 ¹⁹	M	31.3	CR	189 C>A	Tyr63stop	PTC 1-3'
19 ¹⁹	M	NA	NA	90-91 del AG	Frame shift at codon 30, stop at codon 38	PTC 1-5'
20 ¹⁹	F	114.0	Early death	187 ins T	Frame shift at codon 63, stop at codon 67	PTC 1-3'
21 ²⁵	F	26.0	Evolved to ML-DS	194 ins 20 bp GGCCTGGCCTACTACAGGG	Frame shift at codon 65, stop at codon 143	PTC 2
22 ²⁵	F	25.0	Evolved to ML-DS	194 ins 20 bp GGCCTGGCCTACTACAGGG	Frame shift at codon 65, stop at codon 143	PTC 2
23	F	49.9	CR	3 G>T	No translation from Met1	Loss of 1st Met
24	F	46.2	NA	IVS1 3' boundary AG>AA	Splice mutant	Splicing error
25	F	10.5	CR	194 ins 19 bp GCACTGGCCTACTACAGGG	Frame shift at codon 65, stop at codon 73	PTC 1-3'
26 ²⁴	F	244.0	Evolved to ML-DS	1 A>G	No translation from Met1	Loss of 1st Met
27	F	38.3	CR	Loss of 2nd Exon	Splice mutant	Splicing error
28 ²⁴	F	34.6	CR	IVS1 to exon2 del 148 bp	Splice mutant	Splicing error
29	M	25.9	Evolved to ML-DS	160 ins TC	Frame shift at codon 54, stop at codon 137	PTC 2
30	F	52.3	Evolved to ML-DS	187 ins CCTAC	Frame shift at codon 63, stop at codon 138	PTC 2
31 ²⁴	F	221.0	CR	183-193 del 11 bp CTACTACAGGG	Frame shift at codon 62, stop at codon 63	PTC 1-3'
32	M	149.7	CR	2 T>G	No translation from Met1	Loss of 1st Met
33 ²⁴	M	132.3	Evolved to ML-DS	101-108 del 8 bp TCCCCTCT	Frame shift at codon 34, stop at codon 36	PTC 1-5'
34 ²⁴	F	220.0	Early death	90-91 del AG	Frame shift at codon 30, stop at codon 38	PTC 1-5'
35 ²⁴	M	166.0	Early death	IVS2 5' boundary GT>CT	Splice mutant	Splicing error
36 ²⁴	M	57.6	Early death	193-199 GACGCTG>TAGTAGT	Asp65stop	PTC 1-3'
37 ²⁴	M	247.6	Early death	Exon2 to IVS2 del 218 bp	Splice mutant	Splicing error
38 ²⁴	M	93.3	Early death	IVS1 3' boundary AG>AA	Splice mutant	Splicing error
39 ²⁴	M	290.8	Early death	186 ins 12 bp GGCCTGGCCTA	Tyr62stop	PTC 1-3'
40	F	7.8	CR	2 T>C	No translation from Met1	Loss of 1st Met
41 ²⁴	M	136.6	Early death	IVS2 5' boundary GT>GC	Splice mutant	Splicing error
42	M	33.1	Early death	187 ins 8 bp TGGCCTAC	Frame shift at codon 63, stop at codon 139	PTC 2
43	M	9.0	CR	22 ins G	Frame shift at codon 8, stop at codon 39	PTC 1-5'
44	M	24.1	Evolved to ML-DS	149 ins 20 bp AGCAGCTTCTCCACTGCC	Frame shift at codon 50, stop at codon 143	PTC 2
45 ²⁴	F	53.3	CR	173 C>TGCTGCAGTGTAGTA	Frame shift at codon 58, stop at codon 141	PTC 2
46	F	119.0	CR	1 A>C	No translation from Met1	Loss of 1st Met
47	M	33.0	CR	189 C>A	Tyr63stop	PTC 1-3'
48	M	178.2	Early death	188 ins 22 bp GCAGCTGCGGCACCTGGCCTACT	Frame shift at codon 63, stop at codon 74	PTC 1-3'
49	F	73.6	CR	3 G>A	No translation from Met1	Loss of 1st Met
50	F	12.9	CR	158 ins 7 bp AGCACAG	Frame shift at codon 53, stop at codon 69	PTC 1-5'
51	M	13.0	CR	154-161 del 8 bp ACAGCCAC	Frame shift at codon 52, stop at codon 64	PTC 1-5'
52	M	105.5	Early death	4 G>T	Glu2stop	PTC 1-5'
53	F	98.3	CR	4 G>T	Glu2stop	PTC 1-5'
54	F	356.9	CR	219 A>C	Splice mutant	Splicing error
55	F	25.8	Evolved to ML-DS	157 ins CA	Frame shift at codon 53, stop at codon 137	PTC 2
56	M	97.4	Evolved to ML-DS	185-188 del 4 bp ACTA	Frame shift at codon 62, stop at codon 135	PTC 2
57	F	97.3	Early death	3 G>A	No translation from Met1	Loss of 1st Met
58	M	NA	CR	3 G>A	No translation from Met1	Loss of 1st Met
59	M	20.2	CR	150 ins 5 bp TGGCT	Frame shift at codon 50, stop at codon 52	PTC 1-5'
60	M	133.4	CR	174 ins 19 bp CAAAGCAGCTGCAGCGGTG	Frame shift at codon 58, stop at codon 73	PTC 1-3'
61	M	NA	CR	220 G>T	Splice mutant	Splicing error
62	M	120.2	CR	220 G>A	Splice mutant	Splicing error
63	F	39.0	CR	97-139 del 43 bp	Frame shift at codon 33, stop at codon 122	PTC 2
64	F	NA	NA	156 ins C	Frame shift at codon 52, stop at codon 67	PTC 1-5'
65	F	32.4	CR	174 ins 7 bp CTGCAGC	Frame shift at codon 58, stop at codon 69	PTC 1-3'
66	M	69.4	Early death	174-177 GGC A>TGCGGTGG	Frame shift at codon 58, stop at codon 68	PTC 1-3'

We previously reported the GATA1 mutations of the indicated patients.

F indicates female; M, male; CR, complete remission; NA, not available; and IVS, intervening sequence.

*For cDNA nucleotide numbering, nucleotide number 1 corresponds to the A of the ATG translation initiation codon in the reference sequence.

Table 2. GATA1 expression vectors used in this study

Name	Patient no.	GATA1 mutation*	Last normal GATA1 amino acid	PTC	Mutation type
WG	—	—	Ser413	—	Normal
SP1	24, 38	intron1 3' boundary AG>AA	Ser413	—	Splicing error
SP2	41	intron2 5' boundary GT>GC	Ser413	—	Splicing error
L	46	1 A>C	(Met1 is replaced by Val1)	—	Loss of 1st Met
P1-1	11, 19, 34	90, 91 del AG	Gly31	38	PTC 1-5'
P1-2	14, 16, 18, 47	189 C>A	Tyr62	63	PTC 1-3'
P1-3	25	194 ins 19 bp	Arg64	73	PTC 1-3'
P1-4	17	38, 39 del AG	Ser12	38	PTC 1-5'
P1-5	33	101-108 del 8 bp	Phe33	36	PTC 1-5'
P1-6	50	158 ins 7 bp	Tyr52	69	PTC 1-5'
P1-7	3	174 ins 19 bp	Ala58	73	PTC 1-3'
P1-8	48	188 ins 22 bp	Tyr62	74	PTC 1-3'
P2-1	21, 22	194 ins 20 bp	Arg64	143	PTC 2
P2-2	44	149 ins 20 bp	Ala49	143	PTC 2
P2-3	29	160 ins TC	Ala53	137	PTC 2

— indicates not applicable.

*For cDNA nucleotide numbering, nucleotide number 1 corresponds to the A of the ATG translation initiation codon in the reference sequence.

in cells transfected with PTC type 2 constructs, whereas the mRNA levels in mutants that had lost the first methionine and PTC type 1 mutants were almost comparable to those of control minigene constructs harboring wild type *GATA1* gene (Figure 2Aiii). Thus, abundant proteins were produced from *GATA1* mRNAs in mutants with splicing errors and those that lost the first methionine. Conversely, relatively low levels of protein were produced by PTC type 2 mutants because of inefficient translation and reduced levels of message (Figure 2Aiii). However, in the case of PTC type 1 mutations, especially P1-1 and P1-4, we could find no correlation between the amount of transcripts or translation efficiency and the expression levels of GATA1s proteins (Figure 2Aiii).

GATA1s expression levels largely depend on the amount of the alternative splicing form

To investigate the precise relationship between PTC type 1 mutations and GATA1s protein levels, we examined more type 1 mutations

using the minigene constructs. Western blot analysis showed relatively higher expression of the proteins in samples expressing P1-5, P1-7, P1-8, P1-2, and P1-3 than the other constructs (Figure 2Bi). Each mutation in the mutant minigene construct is described in Table 2. Interestingly, all samples that expressed higher levels of GATA1s protein exhibited intense signals at lower molecular weights than the dominant GATA1 signal (Figure 2Biii). Because the size of the lower molecular weight band was identical to that observed in the splicing error mutant (Figure 2Biii), we speculated that the signal might be derived from a transcript lacking exon 2 (Δ exon 2) by alternative splicing. To examine that possibility, we attempted Northern blot analysis using the *GATA1* exon 2 fragment as a probe, and as expected, only the longer transcript was detected (Figure 2Biv). To confirm the correlation between the amount of Δ exon 2 transcript and GATA1s protein, we performed a quantitative assessment by densitometric analysis. The results showed a strong correlation between Δ exon 2 transcript and GATA1s protein

Table 3. Findings at diagnosis and during the course of TAM were significantly associated with early death and the progression to leukemia (univariate analysis)

Variable	Total (n = 66)	Early death (n = 16)	P	Progressed to ML-DS (n = 11)	P
Sex					
Male, n (%)	32 (48.5)	11 (68.8)		5 (45.5)	
Female, n (%)	34 (51.5)	5 (31.3)	.088	6 (54.5)	.947
Median gestational age, wk (range)	37.35 (30.0-40.6)	34.6 (30.0-38.4)		38.1 (32.6-40.6)	
Term versus preterm					
Term (\geq 37 weeks), n (%)	27 (58.7)	4 (30.8)		5 (71.4)	
Preterm (< 37 weeks), n (%)	19 (41.3)	9 (69.2)	.021	2 (28.6)	.465
Median birth weight, kg (range)	2.5 (1.4-3.5)	2.2 (1.6-2.7)		2.5 (1.6-3.5)	
Not LBW versus LBW					
Not LBW (\geq 2.5 kg), n (%)	24 (52.2)	3 (23.1)		3 (42.9)	
LBW (< 2.5 kg), n (%)	22 (47.8)	10 (76.9)	.025	4 (57.1)	.184
Median WBC, $\times 10^9/L$ (range)	69.4 (7.8-423.0)	104.3 (33.1-290.8)		26 (14.6-244.0)	
WBC < 70 $\times 10^9/L$ vs WBC > 70 $\times 10^9/L$					
WBC < 70 $\times 10^9/L$, n (%)	30 (50.8)	4 (25.0)		7 (63.6)	
WBC > 70 $\times 10^9/L$, n (%)	29 (49.2)	12 (75.0)	.020	4 (36.4)	.755
Median peripheral blasts, % (range)	56.0 (4.0-94.0)	78.0 (8.0-93.0)	.031	49.5 (6.0-66.0)	.752
Median AST, IU/L (range)	61 (16-4341)	79 (41-3866)	.620	51 (16-153)	.553
Median ALT, IU/L (range)	39 (4-653)	41 (7-473)	.455	12 (4-96)	.615
Median T-Bil mg/dL (range)	6.3 (0.6-46.0)	6.06 (2.4-16.5)	.922	3.01 (1.82-6.50)	.023
Effusions, n (%)	16 of 44 (36.4)	8 of 11 (72.7)	.007	1 of 7 (14.3)	.912
Bleeding diatheses, n (%)	13 of 45 (28.9)	8 of 12 (66.7)	.001	1 of 7 (14.3)	.123

Some clinical data were not available. We defined the number of patients for whom clinical data was available as (n). LBW indicates low birth weight; AST, aspartate transaminase; ALT, alanine transaminase; and T-Bil, total bilirubin.

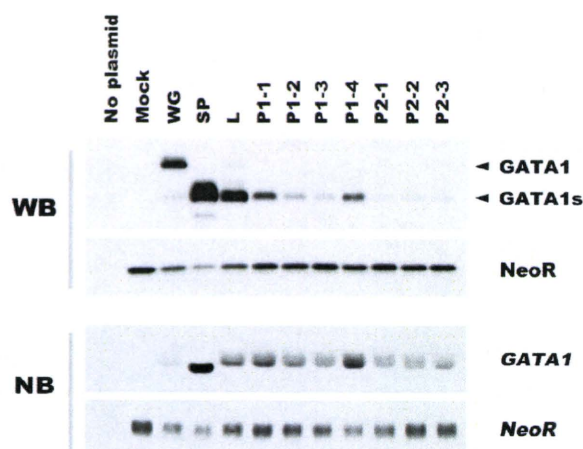


Figure 1. Effects of mutant transcripts of *GATA1* on the expression level of the truncated protein. The *GATA1* mutations observed in TAM patients are classified according to the types of transcripts. The translational efficiency of each transcript was assessed by Western blot analysis in BHK-21 cells transfected with *GATA1* cDNA expression vectors (top part of the panel) and Northern blot analysis (bottom part of the panel), respectively. WG indicates wild type *GATA1*; SP, splicing error mutation (Δ exon 2); L, loss of first methionine mutation; P1, PTC type 1 mutation; P2, PTC type 2 mutation. The details of the *GATA1* mutations are summarized in Table 1. NeoR indicates Neomycin phosphotransferase II.

levels ($r = 0.892$, $P = .003$), but not with the long transcript containing exon 2 nor total *GATA1* mRNA (supplemental Figure 1, available on the *Blood* Web site; see the Supplemental Materials link at the top of the online article). Next, we performed RT-PCR using primers recognizing both transcripts, and calculated the ratio of Δ exon 2 to the long transcript (Figure 2Bvi-vii). The intensive short transcript was detected in all samples with higher expression of *GATA1s* (P1-5, P1-7, P1-8, P1-2, and P1-3; Figure 2Bvii). Interestingly, most of these mutations were clustered in the 3' region of exon 2 (Table 2, Figure 2Bvii). These results suggest that the location of the mutation predicts the efficiency of alternative splicing and *GATA1s* expression levels.

To examine whether differential splicing efficiency could also be observed in TAM blasts with PTC type 1 mutations, RT-PCR analysis was performed using patients' clinical samples. Intense transcription of the short form was observed in the samples from the patients who had *GATA1* mutations located on the 3' side of exon 2 (+169 to +218 in mRNA from the ATG translation initiation codon; Figure 3A-B). We refer to them as PTC type 1-3' and the mutations located on the 5' side of exon 2 as PTC type 1-5'.

Correlation of the phenotype and *GATA1* mutations in TAM patients

Based on these results, *GATA1* mutations were classified into 2 groups: a high *GATA1s* expression group (*GATA1s* high group) including the loss of first methionine type, the splicing error type, and PTC type 1-3', and a low *GATA1s* expression group (*GATA1s* low group) including PTC type 1-5' and PTC type 2. We classified TAM patients into these 2 groups in accordance with the *GATA1s* expression levels estimated from the mutations and compared their clinical data. High counts of WBC and blast cells were significantly associated with the *GATA1s* high group ($P = .004$ and $P = .008$, respectively; Table 4). Although high WBC count was correlated with early death, there were no significant differences in the cumulative incidence of early death between the 2 groups (Figure 4). Importantly, TAM patients in the *GATA1s* low group had a

significantly higher risk for the development of leukemia ($P < .001$; Figure 4). Of 11 TAM patients who progressed to ML-DS, 10 belonged to the *GATA1s* low group. Notably, 8 patients among them had PTC type 2 mutations (Tables 1, 5).

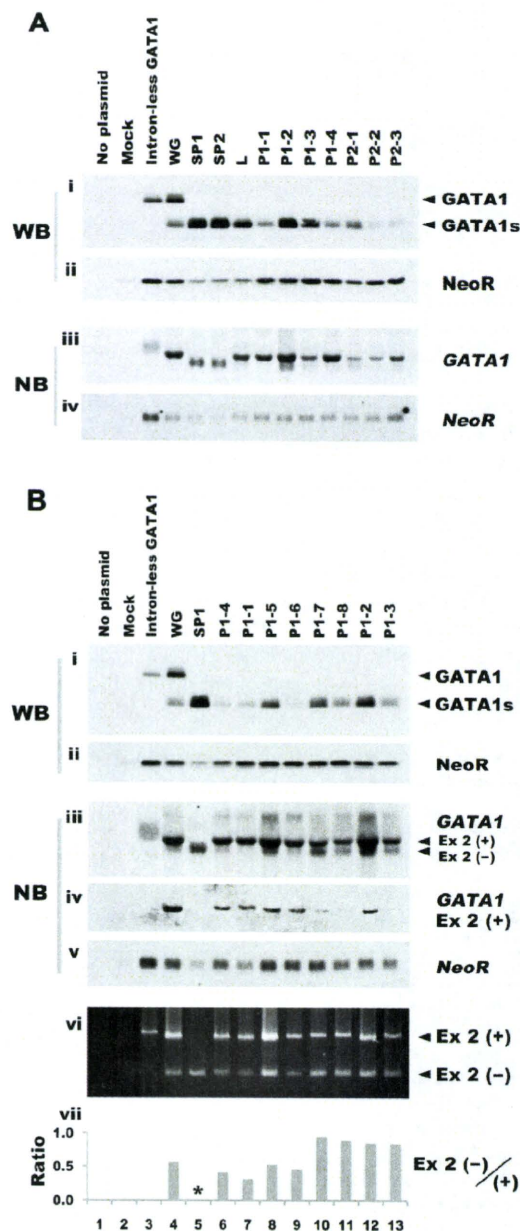


Figure 2. *GATA1* mutations affect the expression level of the truncated protein. (A) The expression levels of *GATA1s* protein and mRNA were assessed in BHK-21 cells transfected with human *GATA1* minigene expression vectors carrying mutations observed in TAM patients. Western blot analysis was performed with anti-*GATA1* (i) or anti-NeoR antibody (ii). Northern blot analysis was carried out with *GATA1* exon 3-6 fragment (iii) or *NeoR* cDNA (iv) as probe. (B) The expression levels of *GATA1s* protein and mRNA in BHK-21 cells transfected with human *GATA1* minigene expression vectors with PTC type 1 mutation. Levels were assessed by Western blot analysis with anti-*GATA1* antibody (i), anti-NeoR antibody (ii). Northern blot analysis was performed with *GATA1* exon 3-6 (iii), exon 2 (iv), or *NeoR* cDNA (v). To detect the transcripts derived from the human *GATA1* minigene expression construct, RT-PCR analysis was carried out using primers described in "RT-PCR" (vi). Ex 2(+) and Ex 2(-) indicate PCR products or transcripts with or without exon 2, respectively. Ratio of Ex 2(-)/(+) was calculated from the results of a densitometric analysis of the RT-PCR. The asterisk denotes unavailable data (vii).

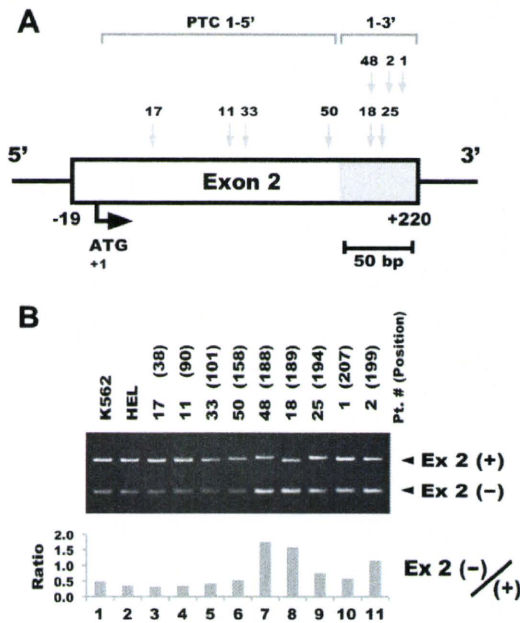


Figure 3. The location of the PTC type 1 mutation affects the efficiency of alternative splicing in TAM blast cells. (A) The location of the *GATA1* mutation in each TAM patient. Details of the mutation in each sample are described in Table 1. (B) RT-PCR analysis of *GATA1* in TAM blast cells harboring PTC type 1 mutations. RT-PCR was performed using primers recognizing both the long transcript including exon 2 and Δ exon 2 (top). All of the patient samples consisted of mononuclear cells from peripheral blood. The numbers in parentheses indicate the number of nucleotides in mRNA from the translation initiation codon. Ex 2(+) and Ex 2(-) indicate PCR products with or without exon 2, respectively (middle). Ratio of Ex 2(-)/(+) was calculated from the results of a densitometric analysis of the RT-PCR (bottom). Note that the intense bands of the short form were observed in the samples from the patients who have *GATA1* mutations located on the 3' side of exon 2 (lanes 7-11).

To validate this observation, we examined the proportion of mutation types in 40 ML-DS patients observed in the same period of time as this surveillance. The results showed a significantly higher incidence of *GATA1*s low type mutations in ML-DS than in TAM ($P = .039$; Table 5). These results further support the present findings that quantitative differences in the mutant protein have a significant effect on the risk of progression to ML-DS.

Table 4. Correlations between patient covariates and *GATA1* expression levels

	GATA1s expression group		P
	High (n = 40)	Low (n = 26)	
Sex: male/female, n	19/21	13/13	.843*
Gestational age, wk	37.3 (30.0-40.0)	37.9 (32.6-40.6)	.487
Birth weight, kg	2.5 (1.6-3.3)	2.5 (1.4-3.5)	.698
WBC, $\times 10^9/L$	105.65 (7.8-423.0)	39.0 (9.0-220.0)	.004
Number of blasts, $\times 10^9/L$	72.1 (0.42-301.6)	13.4 (0.45-189.2)	.008
AST, IU/L	68.5 (23-501)	46.5 (16-4341)	.113
ALT, IU/L	41.0 (5-407)	12.5 (4-653)	.075
T-Bil mg/dL	6.7 (0.6-15.3)	4.65 (1.82-46.0)	.270
Effusions, n (%)	11 of 27 (40.7)	5 of 17 (29.4)	.447†
Bleeding diatheses, n (%)	8 of 29 (27.6)	5 of 16 (31.3)	.528†

Values are given as the median (range). P values estimated by Mann-Whitney U test.

*Pearson χ^2 test.

†Fisher exact test.

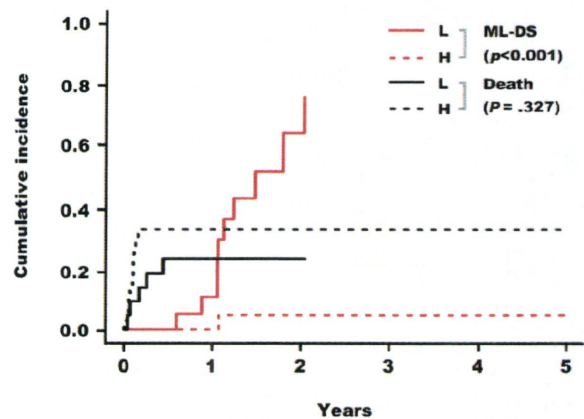


Figure 4. Cumulative incidence of early death and of ML-DS in children with TAM. Based on the estimated *GATA1*s expression levels, patients were classified in 2 groups: *GATA1*s high and low groups. TAM patients in the *GATA1*s low group had a significantly higher risk for the development of leukemia (P (gray) $< .001$).

Discussion

In TAM, *GATA1* mutations lead to the expression of proteins lacking the N-terminal transactivation domain. In addition to this qualitative change, we showed here that the mutations affect the expression level of the truncated protein. The mutations were classified into 2 groups according to the estimated *GATA1*s expression level. Comparison of the clinical features between the 2 groups revealed that *GATA1*s low mutations were significantly associated with a high risk of progression to ML-DS and lower counts of both WBC and blast cells. These results suggest that quantitative differences in protein expression caused by *GATA1* mutations have significant effects on the phenotype of TAM.

*GATA1*s was shown previously to be produced from wild-type *GATA1* through 2 mechanisms: use of the alternative translation initiation site at codon 84 of the full-length transcript and alternative splicing of exon 2.^{12,26} However, the translation efficiencies of *GATA1*s from the full-length of mRNA and short transcripts have not been investigated. Our results clearly showed that the Δ exon 2 transcript produced *GATA1*s much more abundantly than did the full-length transcript. The translation efficiencies of *GATA1*s from full-length transcripts containing PTC were also lower than the alternative spliced form. These results support our contention that *GATA1*s expression levels largely depend on the amount of the Δ exon 2 transcript. Thus, one cannot predict the expression level of *GATA1*s protein from the total amount of the transcript.

The differences in the quantities of *GATA1*s proteins expressed by PTC type 1-5' and -3' mutations revealed the importance of the location of the mutation for splicing efficiency and protein expression. The splicing efficiency is regulated by *cis*-elements located in exons and introns (referred to as exonic and intronic splicing enhancers or silencers), and transacting factors recognizing these elements.^{27,28} The PTC type 1-3' mutations induced efficient skipping of exon 2 (Figures 2Bvi-vii, 3A-B). These mutations might affect exonic splicing enhancers or silencers located in exon 2. To predict the splicing pattern from the mutations more accurately, the elucidation of *cis*-elements and transacting splicing factors, which regulate the splicing of exon 2 of *GATA1*, will be very important.

Table 5. Summary of outcomes and *GATA1* mutation types in TAM patients

Mutation type	Outcome of TAM				TAM		ML-DS	
	CR	Early death	Evolved to ML-DS	NA	Total (n = 66)		Total (n = 40)	
High group								
Loss of 1st Met, n (%)	7	1	1	1	10 (15.2)		3 (7.5)	
Splicing error, n (%)	7	4	0	2	13 (19.7)	40 (15.2)	6 (15.0)	16 (40.0)
PTC 1-3', n (%)	10	6	0	1	17 (25.8)		7 (17.5)	
Low group								
SPTC 1-5', n (%)	6	4	2	3	15 (22.7)	26 (39.4)	14 (35.0)	24 (60.0)
PTC 2, n (%)	2	1	8	0	11 (16.7)		10 (25.0)	

The nonsense mediated RNA decay pathway (NMD), a cellular mechanism for detection of PTC and prevention of translation from aberrant transcripts,^{29,30} might regulate the expression of *GATA1*s protein derived from PTC type 2 mutations, which contained PTCs after the second methionine at codon 84. We consistently detected low amounts of transcripts of *GATA1* in samples expressing PTC type 2 mutations, whereas the expression levels of *GATA1* mRNA from PTC type 1 mutations were comparable with that from wild-type *GATA1* (Figure 2Aiii). These results suggest that the location of PTC relative to alternative translation initiation sites is important for effective NMD surveillance.

Available evidence indicates that acute leukemia arises from cooperation between one class of mutations that interferes with differentiation (class II mutations) and another class that confers a proliferative advantage to cells (class I mutations).³¹ Recent reports showed that introducing high levels of exogenous *GATA1* lacking the N-terminus did not reduce the aberrant growth of *GATA1*-null megakaryocytes, but instead induced differentiation.^{32,33} This observation suggested that abundant *GATA1*s protein functions like a class I mutation in TAM blasts. In contrast, reducing *GATA1* expression leads to differentiation arrest and aberrant growth of megakaryocytic cells.^{19,20} The present data suggest that *GATA1*s is expressed at very low levels in TAM blasts with *GATA1*s low mutations. These levels may not be sufficient to provoke normal maturation. Together, these findings suggest that the low expression of *GATA1*s might function like class II mutations in TAM blasts. Additional class I mutations or epigenetic alterations might be more effective in the development of leukemia in blast cells expressing *GATA1*s at low levels.

In the present study, we identified a subgroup of TAM patients with a higher risk of developing ML-DS. Of 66 children, 11 (16.7%) with TAM subsequently developed ML-DS and 10 of them belonged to the *GATA1*s low group harboring the PTC type 2 or PTC type 1-5' mutations. Surprisingly, 8 of 11 patients (73%) with the PTC type 2 mutations developed ML-DS (Tables 1, 5), whereas 2 of 15 patients (13.3%) with PTC type 1-5' mutations developed leukemia. The estimated expression levels of *GATA1*s from PTC type 2 mutations were lower than those from PTC type 1-5' mutations (Figures 1, 2Ai). These results suggest that the type 2 mutations may be a more significant risk factor for developing ML-DS (supplemental Figure 2). However, our classification of *GATA1* mutations mainly rested on extrapolation from in vitro transfection experiments (Figures 1-2) and RT-PCR analyses of a small number of patient samples (Figure 3). The stability of the transcripts and the splicing efficiency of the second exon of *GATA1* will be regulated through complex mechanisms. To confirm our findings, precise mapping of the mutations that affect the expres-

sion levels of *GATA1*s and a prospective study with a large series of TAM patients are necessary.

Finally, we proposed the hypothesis that the quantitative differences in *GATA1*s protein expression caused by mutations have a significant effect on the phenotype of TAM. The observations described here provide valuable information about the roles of *GATA1* mutations on multistep leukemogenesis in DS patients. Moreover, the results might have implications for management of leukemia observed in DS infants and children. Because the blast cells in both TAM and subsequent ML-DS appear highly sensitive to cytarabine,³⁴⁻³⁹ the preleukemic clone could be treated with low-dose cytarabine without severe side effects, and elimination of the preleukemic clone might prevent progression to leukemia.

Acknowledgments

We thank Dr Tetsuo Mitsui (Yamagata University School of Medicine), Shingo Morinaga (National Hospital Organization Kumamoto Medical Center), Takahide Nakano (Kansai Medical University), Masahiro Migita (Japan Red Cross Kumamoto Hospital), Hiroshi Kanda (Kurume University School of Medicine), Koji Kato (The First Nagoya Red Cross Hospital), and Takahiro Uehara (Kameda Medical Center) for providing patient samples. We thank Dr Eiki Tsushima, Ko Kudo (Hirosaki University Graduate School of Medicine), and Ms Hitomi Iwabuchi for statistical analysis, helpful discussions, and technical assistance, respectively.

This work was supported by grants-in-aid from the Ministry of Education, Culture, Sports, Science, and Technology of Japan and Health and Labor Sciences Research Grants (research on intractable diseases) the Ministry of Health, Labor, and Welfare of Japan.

Authorship

Contribution: R.K. and T. Toki designed, organized, and performed research, analyzed data, and wrote the paper; K.T. designed research and collected and analyzed clinical data; G.X. and R.W. performed mutation screening; A.S., H.K., K. Kawakami, M.E., D.H., K. Kogawa, S.A., Y.I., S.I., T. Taga, Y.K., and Y.H. provided clinical samples and data; A.H. and S.K. performed mutation screening and provided clinical samples and data; and E.I. designed and organized research, analyzed data, and wrote the paper.

Conflict-of-interest disclosure: The authors declare no competing financial interests.

Correspondence: Etsuro Ito, Department of Pediatrics, Hirosaki University Graduate School of Medicine, 5 Zaifu-cho, Hirosaki, Aomori, 036-8563, Japan; e-mail: etrou@cc.hirosaki-u.ac.jp.

References

- Zipursky A, Poon A, Doyle J. Leukemia in Down syndrome: a review. *Pediatr Hematol Oncol*. 1992;9(2):139-149.
- Hasle H, Niemeyer CM, Chessells JM, et al. A pediatric approach to the WHO classification of myelodysplastic and myeloproliferative diseases. *Leukemia*. 2003;17(2):277-282.
- Hitzler JK. Acute megakaryoblastic leukemia in Down syndrome. *Pediatr Blood Cancer*. 2007;49(7):1066-1069.
- Malinge S, Izraeli S, Crispino JD. Insights into the manifestations, outcomes, and mechanisms of leukemogenesis in Down syndrome. *Blood*. 2009;113(12):2619-2628.
- Massey GV, Zipursky A, Chang MN, et al. A prospective study of the natural history of transient leukemia (TL) in neonates with Down syndrome (DS): Children's Oncology Group (COG) study POG-9481. *Blood*. 2006;107(12):4606-4613.
- Klusmann JH, Creutzig U, Zimmermann M, et al. Treatment and prognostic impact of transient leukemia in neonates with Down syndrome. *Blood*. 2008;111(6):2991-2998.
- Muramatsu H, Kato K, Watanabe N, et al. Risk factors for early death in neonates with Down syndrome and transient leukaemia. *Br J Haematol*. 2008;142(4):610-615.
- Wechsler J, Greene M, McDevitt MA, et al. Acquired mutations in GATA1 in the megakaryoblastic leukemia of Down syndrome. *Nat Genet*. 2002;32(1):148-152.
- Greene ME, Mundschaug G, Wechsler J, et al. Mutations in GATA1 in both transient myeloproliferative disorder and acute megakaryoblastic leukemia of Down syndrome. *Blood Cells Mol Dis*. 2003;31(3):351-356.
- Hitzler JK, Cheung J, Li Y, Scherer SW, Zipursky A. GATA1 mutations in transient leukemia and acute megakaryoblastic leukemia of Down syndrome. *Blood*. 2003;101(11):4301-4304.
- Mundschaug G, Gurbuxani S, Gamis AS, Greene ME, Arceci RJ, Crispino JD. Mutagenesis of GATA1 is an initiating event in Down syndrome leukemogenesis. *Blood*. 2003;101(11):4298-4300.
- Rainis L, Bercovich D, Strehl S, et al. Mutations in exon 2 of GATA1 are early events in megakaryocytic malignancies associated with trisomy 21. *Blood*. 2003;102(3):981-986.
- Xu G, Nagano M, Kanezaki R, et al. Frequent mutations in the GATA-1 gene in the transient myeloproliferative disorder of Down syndrome. *Blood*. 2003;102(8):2960-2968.
- Groet J, McElwaine S, Spinelli M, et al. Acquired mutations in GATA1 in neonates with Down's syndrome with transient myeloid disorder. *Lancet*. 2003;361(9369):1617-1620.
- Weiss MJ, Orkin SH. Transcription factor GATA-1 permits survival and maturation of erythroid precursors by preventing apoptosis. *Proc Natl Acad Sci U S A*. 1995;92(21):9623-9627.
- Morceau F, Schnekenburger M, Dicato M, Diederich M. GATA-1: friends, brothers, and co-workers. *Ann N Y Acad Sci*. 2004;1030:537-554.
- Ferreira R, Ohneda K, Yamamoto M, Philipsen S. GATA1 function, a paradigm for transcription factors in hematopoiesis. *Mol Cell Biol*. 2005;25(4):1215-1227.
- Gutierrez L, Tsukamoto S, Suzuki M, et al. Ablation of Gata1 in adult mice results in aplastic crisis, revealing its essential role in steady-state and stress erythropoiesis. *Blood*. 2008;111(8):4375-4385.
- Shivdasani RA, Fujiwara Y, McDevitt MA, Orkin SH. A lineage-selective knockout establishes the critical role of transcription factor GATA-1 in megakaryocyte growth and platelet development. *EMBO J*. 1997;16(13):3965-3973.
- Vyas P, Ault K, Jackson CW, Orkin SH, Shivdasani RA. Consequences of GATA-1 deficiency in megakaryocytes and platelets. *Blood*. 1999;93(9):2867-2875.
- Shimizu R, Kuroha T, Ohneda O, et al. Leukemogenesis caused by incapacitated GATA-1 function. *Mol Cell Biol*. 2004;24(24):10814-10825.
- Shimizu R, Engel JD, Yamamoto M. GATA1-related leukaemias. *Nat Rev Cancer*. 2008;8(4):279-287.
- Xu G, Kanezaki R, Toki T, et al. Physical association of the patient-specific GATA1 mutants with RUNX1 in acute megakaryoblastic leukemia accompanying Down syndrome. *Leukemia*. 2006;20(6):1002-1008.
- Toki T, Kanezaki R, Adachi S et al. The key role of stem cell factor/KIT signaling in the proliferation of blast cells from Down syndrome-related leukemia. *Leukemia*. 2009;23(1):95-103.
- Shimada A, Xu G, Toki T et al. Fetal origin of the GATA-1 mutation in identical twins with transient myeloproliferative disorder and acute megakaryoblastic leukemia accompanying Down's syndrome. *Blood*. 2004;103(1):366.
- Calligaris R, Bottardi S, Cogoi S, Apezteguia I, Santoro C. Alternative translation initiation site usage results in two functionally distinct forms of the GATA-1 transcription factor. *Proc Natl Acad Sci U S A*. 1995;92(25):11598-11602.
- Pozzoli U, Sironi M. Silencers regulate both constitutive and alternative splicing events in mammals. *Cell Mol Life Sci*. 2005;62(14):1579-1604.
- Wang Z, Burge CB. Splicing regulation: from a parts list of regulatory elements to an integrated splicing code. *FNA*. 2008;14(5):802-813.
- Neu-Yilik G, Kulozik AE. NMD: multitasking between mRNA surveillance and modulation of gene expression. *Adv Genet*. 2008;62:185-243.
- Shyu AB, Wilkinson MF, van Hoof A. Messenger RNA regulation: to translate or to degrade. *EMBO J*. 2008;27(3):471-481.
- Deguchi K, Gilliland DG. Cooperativity between mutations in tyrosine kinases and in hematopoietic transcription factors in AML. *Leukemia*. 2002;16(4):740-744.
- Kuhl C, Atzberger A, Iborra F, Nieswandt B, Porcher C, Vyas P. GATA1-mediated megakaryocyte differentiation and growth control can be uncoupled and mapped to different domains in GATA1. *Mol Cell Biol*. 2005;25(19):8592-8606.
- Muntean AG, Crispino JD. Differential requirements for the activation domain and FOG-interaction surface of GATA-1 in megakaryocyte gene expression and development. *Blood*. 2005;106(4):1223-1231.
- Taub JW, Matherly LH, Stout ML, Buck SA, Gurney JG, Ravindranath Y. Enhanced metabolism of 1-beta-D-arabinofuranosylcytosine in Down syndrome cells: a contributing factor to the superior event free survival of Down syndrome children with acute myeloid leukemia. *Blood*. 1996;87(8):3395-3403.
- Taub JW, Huang X, Matherly LH, et al. Expression of chromosome 21-localized genes in acute myeloid leukemia: differences between Down syndrome and non-Down syndrome blast cells and relationship to in vitro sensitivity to cytosine arabinoside and daunorubicin. *Blood*. 1999;94(4):1393-1400.
- Frost BM, Gustafsson G, Larsson R, Nygren P, Lonnholm G. Cellular cytotoxic drug sensitivity in children with acute leukemia and Down's syndrome: an explanation to differences in clinical outcome? *Leukemia*. 2000;14(5):943-944.
- Zwaan CM, Kaspers GJ, Pieters R, et al. Different drug sensitivity profiles of acute myeloid and lymphoblastic leukemia and normal peripheral blood mononuclear cells in children with and without Down syndrome. *Blood*. 2002;99(1):245-251.
- Ge Y, Stout ML, Tatman DA, et al. GATA1, cytidine deaminase, and the high cure rate of Down syndrome children with acute megakaryocytic leukemia. *J Natl Cancer Inst*. 2005;97(3):226-231.
- Taub JW, Ge Y. Down syndrome, drug metabolism and chromosome 21. *Pediatr Blood Cancer*. 2005;44(1):33-39.

Expression of ADAMTS4 in Ewing's sarcoma

K. MINOBE^{1,2}, R. ONO^{1*}, A. MATSUMINE^{3*}, F. SHIBATA-MINOSHIMA², K. IZAWA²,
T. OKI², J. KITAURA², T. IINO³, J. TAKITA⁴, S. IWAMOTO⁵, H. HORI⁵, Y. KOMADA⁵,
A. UCHIDA³, Y. HAYASHI⁶, T. KITAMURA² and T. NOSAKA¹

¹Department of Microbiology and Molecular Genetics, Mie University Graduate School of Medicine, Tsu; ²Division of Cellular Therapy, The Institute of Medical Science, The University of Tokyo, Tokyo; ³Department of Orthopaedic Surgery, Mie University Graduate School of Medicine, Tsu; ⁴Department of Cell Therapy and Transplantation Medicine, Graduate School of Medicine, The University of Tokyo, Tokyo; ⁵Department of Pediatrics and Developmental Science, Mie University Graduate School of Medicine, Tsu; ⁶Gunma Children's Medical Center, Gunma, Japan

Received March 29, 2010; Accepted May 18, 2010

DOI: 10.3892/ijo_00000706

Abstract. Ewing's sarcoma (EWS) is a malignant bone tumor that frequently occurs in teenagers. Genetic mutations which cause EWS have been investigated, and the most frequent one proved to be a fusion gene between *EWS* gene of chromosome 22 and the *FLI1* gene of chromosome 11. However, a limited numbers of useful biological markers for diagnosis of EWS are available. In this study, we identified ADAMTS4 (a disintegrin and metalloproteinase with thrombospondin motifs) as a possible tumor marker for EWS using the retrovirus-mediated signal sequence trap method. ADAMTS4 is a secreted protein of 837 amino acids with a predicted molecular mass of 98-100 kDa. It is a member of metalloprotease family, is expressed mainly in cartilage and brain, and regulates the degradation of aggrecans. ADAMTS4 has been suggested to be involved in arthritic diseases and gliomas. Herein, we show that *ADAMTS4* mRNA was expressed in all primary EWS samples and all EWS-derived cell lines examined, while its expression was detected only in small subpopulations of other solid tumors. Furthermore, *ADAMTS4* expression was found to be regulated by *EWS-FLI1* fusion gene-dependent manner. We also demonstrated that ADAMTS4 protein was highly expressed in tumor samples of the patients with EWS by using immunohistochemistry. These results suggest that ADAMTS4 is a novel tumor marker for EWS.

Introduction

Ewing's sarcoma (EWS) is the second most frequent primary bone tumor of childhood and adolescence with aggressive clinical course and poor prognosis. It is recognized that EWS is a part of Ewing's sarcoma family of tumors (ESFTs) which also include the peripheral primitive neuroectodermal tumor (PNET) (1,2), Askin's tumor and extraosseous EWS. Biologically, ESFTs are characterized by common chromosomal translocation between the 5' portion of the *EWS* gene (22q12) and the 3' portion of the members of the *ETS* family genes (3). More than 85% of the cases have the fusion gene *EWS-FLI1* due to t(11;22)(q24;q12) (4,5). Five to 10% of the cases possess *EWS-ERG* due to t(21;22)(q22;q12) (6). The other rare cases are *EWS-ETV1*, *EWS-E1AF* and *EWS-FEV*, each resulting from t(7;22)(p22;q12), t(17;22)(q12;q12) and t(2;22)(q33;q12), respectively (3,7,8). The EWS-ETS chimeric proteins behave as aberrant transcriptional regulators and are believed to play a crucial role in the onset and progression of the ESFTs (9,10).

Currently, diagnosis of EWS is determined mainly by CD99 immunohistochemistry (11-13), and by genetic aberration. However, CD99 expression is also reported to be positive in some T cell acute lymphoblastic leukemia (T-ALL), acute myelogenous leukemia (AML), ependymoma, synovial sarcoma and pancreatic endocrine tumors (14-16). Besides, not all EWSs have this specific chromosomal translocation. Thus, there is no specific biomarker for differentiating EWS from other soft tissue sarcomas. Among the patients with localized tumor at diagnosis, 20% relapse within 4 years and die of the disease. In contrast, 5-year survival rate is ~20-30% in cases with metastasis. This study was performed to find a useful tumor marker for EWS.

The signal sequence trap (SST) is a strategy to identify complementary DNAs (cDNAs) containing signal sequence that encode secreted and type I membrane proteins (17). To date, various important molecules have been detected including *SDF-1*, a member of the tumor necrosis factor receptor superfamily *TROY*, *Xenopus-Tsukushi*, *Vasorin* and leukocyte mono-Ig-like receptor (*LMIR*) by the SST method

Correspondence to: Dr T. Nosaka, Department of Microbiology and Molecular Genetics, Mie University Graduate School of Medicine, 2-174, Edobashi, Tsu 514-8507, Japan
E-mail: nosaka@doc.medic.mie-u.ac.jp

*Contributed equally

Key words: EWS-FLI1, tumor marker, signal sequence trap, retrovirus

(18-23). In this study, we identified a secreted molecule *ADAMTS4* (a disintegrin and metalloproteinase with thrombospondin motifs) from EWS cell lines by using the SST system based on retrovirus-mediated expression screening (SST-REX) (24,25).

ADAMTS is a family of proteinases which was first described in 1997 (26). Today, 19 different members of the *ADAMTS* family have been identified, but the functions, mechanisms of activation, and substrates of most members remain incompletely understood (27). Members of the *ADAMTS* family are closely related to the *ADAM* (a disintegrin and metalloproteinase) family, but unlike *ADAMs*, the *ADAMTSs* are secreted molecules, some of which bind to the extracellular matrix. *ADAMTS4* was originally purified from chondrocytes and synovial cells stimulated with interleukin-1 (28). The structure of *ADAMTS4* consists of six domains, a prodomain, a metalloproteinase domain, a disintegrin domain, a thrombospondin type I motif, a cysteine-rich domain and a spacer domain. It has been demonstrated to cleave the aggrecan at Glu³⁷³-Ala³⁷⁴, and therefore is also named as *aggrecanase1* (29-32). The aggrecanase activity of *ADAMTS4* is inhibited by TIMP-3 (tissue inhibitor of metalloproteinase-3) (33), which was originally identified as an inhibitor of matrix metalloproteinases. Yamanishi *et al* demonstrated that *ADAMTS4* was overexpressed in synovial cells and chondrocytes in the patients with osteoarthritis (OA) and rheumatoid arthritis (RA) (34). Thus, *ADAMTS4* is considered to play an important role in the aggrecan degradation of articular cartilage in OA and RA. Recent studies reported that *ADAMTS4* cleaves not only aggrecan but also brevican, versican and α 2-macroglobulin (35).

In this study, we have disclosed that *ADAMTS4* mRNA was expressed in all tissue samples of EWS patients and all EWS cell lines examined, and the mRNA level of *ADAMTS4* was regulated by *EWS-FLI1* in the cell line. We have also demonstrated the *ADAMTS4* protein expression by immunostaining of the patients' samples and the cell lines. Thus, we propose that *ADAMTS4* is a possible tumor marker of EWS.

Materials and methods

Cell lines. Osteosarcoma cell lines (MG63, HOS, KHOS/NP, SaOS2 and U2OS), neuroblastoma cell lines (KPNSI-FA, LAN-1 and NB69), a lung cancer cell line H460, a liver cancer cell line PLC/PRF/5, a cholangiocarcinoma cell line HuCCT1, a colon cancer cell line SW-48, T-ALL cell lines (Jurkat, PEER, CEM and HPB-ALL), B-ALL cell lines (NALM16, NALM24 and IM9), AML cell lines (MOLM13 and ML1), an acute myelomonocytic leukemia cell line U937, EWS cell lines (SJES-2, SJES-3, SJES-5, SJES-6, SJES-7 and SJES-8), rhabdomyosarcoma cell lines (RMS and SJRH-30), pancreatic cancer cell lines (AsPC-1, BxPC-3 and Capan-1), glioblastoma cell lines (U87MG, U251 and T98G), and gastric cancer cell lines (HGC-27, MKN45, GCIY and KATO-III) were cultured in RPMI-1640 medium (Sigma-Aldrich, St. Louis, MO, USA) containing 10% heat-inactivated fetal bovine serum (FBS) (Sigma-Aldrich). A murine pro-B cell line Ba/F3 was maintained in RPMI-1640 containing 10% FBS and 1 ng/ml murine interleukin-3 (IL-3)

(R&D Systems, Minneapolis, MN, USA). A retrovirus packaging cell line Plat-E (36) and NIH3T3 were cultured in Dulbecco's modified Eagle's medium (DMEM) (Sigma-Aldrich) containing 10% FBS. Human mesenchymal stem/progenitor cells (hMSCs) were purchased from Sanko Junyaku (Tokyo, Japan).

Patient samples and normal controls. Samples from 7 patients with EWS, 13 osteosarcoma, 4 chondrosarcoma, 4 synovial sarcoma, and 3 rhabdomyosarcoma, which were obtained at initial surgery at the department of orthopaedic surgery at Mie University Hospital, were examined by reverse transcription (RT)-PCR. Schwannoma, desmoid and lipoma samples were used as controls. Tissue samples for immunohistochemical staining were obtained from 25 EWS patients who underwent an open biopsy or a surgical resection. For enzyme-linked immunosorbent assay (ELISA), we used serum samples of 3 osteosarcomas, 1 osteofibrous dysplasia, 1 chondrosarcoma, 1 synovial sarcoma, 6 EWS and 4 healthy volunteers. Basically sera were isolated before the chemotherapy except for few cases. Informed consent was obtained from each patient or parent and volunteer. This study was approved by the ethics committee at Mie University.

Antibodies and other reagents. A rabbit polyclonal anti-*ADAMTS4* antibody which was raised against amino acids 764-837 of human *ADAMTS4* (Santa Cruz Biotechnology, Santa Cruz, CA, USA) and a horseradish peroxidase (HRP)-conjugated goat anti-rabbit IgG secondary antibody (Bio-Rad Laboratories, Hercules, CA, USA) were used for immunoprecipitation (IP)-Western blot analysis. Immunostaining was performed by using the following antibodies: the same anti-*ADAMTS4* antibody as used for IP-Western analysis, an N-universal rabbit IgG (Dako, Kyoto, Japan), an HRP-conjugated anti-rabbit IgG antibody (Nichirei Biosciences, Tokyo, Japan) for immunohistochemistry, and an Alexa488-conjugated anti-rabbit IgG antibody (Invitrogen, Carlsbad, CA, USA) for immunofluorescence microscopy. For ELISA, a monoclonal anti-*ADAMTS4* antibody raised against amino acids 213-685 of the recombinant human *ADAMTS4* (R&D Systems), a biotinylated goat anti-*ADAMTS4* antibody raised against amino acids 213-685 of the recombinant human *ADAMTS4* and an Avidin-HRP (eBioscience, San Diego, CA, USA) were used.

Screening of EWS cDNA library by SST. A human EWS cDNA library was screened by SST-REX as previously described (24,25). Briefly, poly(A)⁺ RNA was prepared from EWS cell lines using the FastTrack2.0 Kit (Invitrogen). The cDNA was synthesized from the mixture of poly(A)⁺ RNAs of 6 EWS cell lines with random hexamers, using the SuperScript Choice System (Invitrogen) according to the manufacturer's instructions. The synthesized cDNA was size-separated by electrophoresis on an agarose gel. Fractions greater than 500 bp were collected and inserted into *Bst*XI sites of pMX-SST (25) using *Bst*XI adaptors (Invitrogen). Ba/F3 cells were infected with the retroviruses expressing the EWS-derived cDNA library and selected for growth in the absence of IL-3. Genomic DNAs extracted from IL-3-independent clones were subjected to PCR to recover the

Table I. Primer sequences used in RT-PCR analyses in murine tissues.

Gene	Sense	Antisense
DKFZP56400823	5'-CCATTGCCTGTCTCTCATGACA-3'	5'-GAGCTGTGCTCTTCTGTTGGTGA-3'
ADAMTS4	5'-GAGCTGTGCTCTTCTGTTGGTGA-3'	5'-CAGAGAAGCGAAGCGCTTGGTT-3'
DNER	5'-GACATAATCCTGCCCGCTCT-3'	5'-CTCTGATGGCTTCGTGGCACAT-3'
NGFR	5'-CGTGTCTCTCTGCCAGGACAA-3'	5'-GCTGTGCAGTTTCTCTCCCTCT-3'
LRRN6A	5'-GTCTTCACCGGCCTCAGCAA-3'	5'-CCCTCGATTGTACCGATTGGGTT-3'
ECSM2	5'-GACAACTCAGACCTCGCAGGAA-3'	5'-CATTGGCTGTGGAGCAGCTTTC-3'
LGALS3BP	5'-CAGGACTACTGTGGACGGCTT-3'	5'-CTACTCCAGGTGGAAGAGGTGTA-3'
PTPRF	5'-GCTGGCCCAGGAGAAGAGTT-3'	5'-GCTCTGCCCATGTACAGGATCTT-3'
FCGRT	5'-GCTGTGAACTGGCCTCGGATA-3'	5'-CCAGCAATGACCATGCGTGGAA-3'
LAMP2	5'-CGCTGTCTCTTGGGCTGTGAAT-3'	5'-GGCACCTTCTCCTCAGTGATGTT-3'
RCN1	5'-CTAAGCCCGACGAGAGCAA-3'	5'-GGCCATTGTCTCGTGGGAA-3'
MMP14	5'-CATGAGTTGGGGCATGCCCTA-3'	5'-CGGCCAAGCTCCTTAATGTGCTT-3'
SDC2	5'-CTCCATTGAGGAAGCTTCAGGAGT-3'	5'-CTTCTGGTAAGCTGCGCTGGAT-3'
DAG1	5'-GGAAGCCACGGTCACCATT-3'	5'-GCTTGAGCTTGTCGGTAGTGGTA-3'
EPCR	5'-GGCAACGCCTCTCTGGGAAAA-3'	5'-CGGCCACACCAGCGATTATGAA-3'
CD97	5'-CTGGAACAAAGCCTTCGGACCTT-3'	5'-GTCGGTGTCCCAGTACCCATT-3'
CD99L2	5'-GTCCAGAGAGGATATGGAGACACA-3'	5'-GGTTCTGCAGACTGCGTTTCTTG-3'
IGFBP5	5'-GCGACGAGAAAGCTCTGTCCAT-3'	5'-GCCTTGTTCCGATTCCCTGTCTCA-3'
CLU	5'-GAAGGCATCCCGGAAGTGTGTA-3'	5'-GCTGGACATCCATGGCCTGTT-3'
LSAMP	5'-GCTCTGGAATACAGCCTCCGAA-3'	5'-GTGTCATCCCGGTACCACTCAA-3'
NPTN	5'-GTAACCTCACTCCAGCTCTCACA-3'	5'-GGAGGCAGAGCCAATGGAGTT-3'
EFNA5	5'-GCAGCAACCCCAGATTCCAGA-3'	5'-GATGGCTCGGCTGACTCATGTA-3'
PODXL	5'-CCTTACCAGTAGCAGTGGACAA-3'	5'-CCACTGTAGACGCCATAGACTGT-3'
TMEM123	5'-CCACTCAGTGCTGACCTCCAA-3'	5'-GTTTCGTCAATGCTTCGGTACCGAA-3'
GAPDH	5'-CAGTATGACTCCACTCACGGCAA-3'	5'-CAGATCCACGACGGACACATTG-3'

integrated cDNAs using vector primers. The resulting PCR fragments were sequenced and analyzed.

RT-PCR analysis. RT-PCR was carried out to detect *ADAMTS4* transcript in tumor cell lines, murine tissues and patients' samples. Total RNA was isolated with acid guanidium-phenol-chloroform method, and then 5 µg RNA was reverse-transcribed to cDNA in a total volume of 33 µl with random hexamers by using the Ready-To-Go You-Prime First-Strand Beads (GE Healthcare UK, Buckinghamshire, UK). RT-PCR was performed with the programmable cyclic reactor under the following conditions: denaturation at 94°C for 3 min followed by 30 cycles of amplification (94°C for 30 sec, 60°C for 30 sec, and 72°C for 45 sec). PCR product was separated by 1-2% agarose gel electrophoresis and visualized by ethidium bromide staining. The primers used for RT-PCR was described in Tables I and II.

Cloning of the full-length cDNA encoding *ADAMTS4*. Full-length *ADAMTS4* was generated as follows. The first half of *ADAMTS4* (1-1194 bp) was isolated from pMX-SST vector by digestion with *Bam*HI. Based on the sequence data, the last half (1195-2514 bp) were amplified by PCR from cDNAs of the EWS cell line SJES-5, and digested with *Bam*HI and *Not*I. The fragment was subcloned into a pMXs-puro

retroviral vector (37). The resultant vector was digested with *Bam*HI, and then ligated with the *Bam*HI fragment of the first half of *ADAMTS4*. The primers used for amplification are as follows: SST5', 5'-GGGGGTGGACCATCCTCTA-3'; SST3', 5'-CGCGCAGCTGTAAACGGTAG-3'; ADAMTS4-FL-S, 5'-GAAAGAATTTCGCTGCAGTACCAGTGCCATG-3'; ADAMTS4-FL-S2, 5'-GAGCACCTCTCGCCATGTCA-3'; ADAMTS4-FL-AS, 5'-GAAAGAGAATTTCGCGGCCGCTATTTCTGCCCGCCAGG-3'; ADAMTS4-AS2, 5'-CTTTGGATCCACATGAGCCATCACAGGGGCCATGACATGGCGAGAGGTGCTCAAAGGCCATTCAAATGATGCATG-3'.

Transfection and infection. Retroviral transfection was done as described previously (36,37). Briefly, retroviruses were generated by transient transfection of Plat-E packaging cells (36) with FuGENE 6 (Roche Diagnostics, Basel, Switzerland). Ba/F3 and NIH3T3 cells were infected with the retroviruses in the presence of 10 µg/ml polybrene. Selection with G418 or puromycin was started 48 h after infection.

Small interfering (si)RNA design and transfection experiments. *EWS-FLI1*-specific siRNA (siEF1) for SJES-5 cell line was designed as previously described (38). As a negative control, siGFP was employed (Hayashi-Kasei, Osaka, Japan).

Table II. Primer sequences used in RT-PCR analyses in human cancer cell lines.

Gene	Sense	Antisense
DKFZP56400823	5'-CCATCTGGACTAGCTCTCCACA-3'	5'-GTGCTGGTCACAGTGGAGCTA-3'
ADAMTS4	5'-GTGGAGTCTCCACTTGGGACA-3'	5'-CCAGGGCGAGTGTGGTCT-3'
DNER	5'-GTGGTGAAGGTCAGCACCTGT-3'	5'-GGCTGAGGGCACAGAAGTCAA-3'
NGFR	5'-GTTCTCTGCCAGGACAAGCA-3'	5'-GTCCACGGAGATGCCACTGT-3'
LRRN6A	5'-GTACAACCTCAAGTCACTGGAGGT-3'	5'-CATTGAGCACGCGCAGGTAGTT-3'
ECSM2	5'-CAATGACCCAGACCTCTAGCTCT-3'	5'-GCAGCTTTCAGACAGCCCTGA-3'
LGALS3BP	5'-CCCACAGACCTGCTCCAACCT-3'	5'-CCGTCTGGACTGATAGACCAGTT-3'
PTPRF	5'-CAGCCCCTACTCGGATGAGAT-3'	5'-GCGATGACATTCGCATAGCGGTT-3'
FCGRT	5'-CTCTCCCTCCTGTACCACCTT-3'	5'-GTGCCCTGCTTGAGGTGCAAAT-3'
LAMP2	5'-GTGCAGTTCGGACCTGGCTT-3'	5'-CAGCTGCCTGTGGAGTGAGTT-3'
RCN1	5'-GACAATGATGGGGATGGCTTTGTCA-3'	5'-CGGAATTCGTTAAACTGCTCCCGTT-3'
MMP14	5'-CAACATTGGAGGAGACACCCACTTT-3'	5'-GTTCCAGGGACGCCTCATCAA-3'
SDC2	5'-GCTCCATTGAAGAAGCTTCAGGAGT-3'	5'-GCCTTCTGATAAGCAGCACTGGAT-3'
DAG1	5'-CGGAGGCAGATCCATGCTACA-3'	5'-GGCAGTTTCCAATCTGGTGATGGA-3'
EPCR	5'-CTACTTCCGCGACCCCTATCA-3'	5'-GCGAAGTGTAGGAGCGGCTT-3'
CD97	5'-CAAGACAAGCTCAGCCGAGGT-3'	5'-CTCCCCATCGGAGGACTCAA-3'
CD99L2	5'-CAAGAAACCCAGTGCTGGGGAT-3'	5'-GTACGCTGAACAGCTGGCTCT-3'
IGFBP5	5'-CTCAACGAAAAGAGCTACCGCGA-3'	5'-CTGTGGAAGGTGTGGCACTGAA-3'
CLU	5'-CAATGAGACCATGATGGCCCTCT-3'	5'-CCGGGCTATGGAAGTGATGT-3'
LSAMP	5'-GGACAACATCACCGTGAGGCA-3'	5'-GGAGACCTCGTTGGCAGCTT-3'
NPTN	5'-CCCTGTCACCCTGCAGTGTA-3'	5'-CCAATGGCGTTGGTGGCATTACA-3'
EFNA5	5'-CCAGAGGGGTGACTACCATATTGA-3'	5'-CGGCTGACTCATGTACGGTGT-3'
PODXL	5'-CTCCACAGCCACAGCTAACCTA-3'	5'-CTGGCAGGGTAGGTGTTCTCAA-3'
TMEM123	5'-CCATGGCGGCATCTGCAAACAT-3'	5'-CGATACCGAATGCCTCTTCTTGAGT-3'
PCOLCE	5'-CGGACGCTTTTGTGGGACCTT-3'	5'-GGCAGCTTGACTTTAGGCTCAGTT-3'
SEZ6L2	5'-GCACCTGCACTTTGAAAGGGTCT-3'	5'-GTCCCTTCCCGCACATTCAATAT-3'
IGFBP4	5'-GAAGCCCCTGCACACACTGAT-3'	5'-GAAAGCTGTCAGCCAGCTGGT-3'
IGFBP3	5'-GCATCTACACCGAGCGCTGT-3'	5'-GGGACTCAGCACATTGAGGAACTT-3'
LOX	5'-GTCACTGGTTCGAAGCTGGCTA-3'	5'-GGAATATCTTGGTCGGCTGGGTA-3'
CTGF	5'-GCGTGTGCACCGCCAAAGAT-3'	5'-CGGTATGTCTTCATGCTGGTGCA-3'
SPARC	5'-CTGCCAGAACCACCACTGCAA-3'	5'-CTGCCAGTGTACAGGGAAAGATGT-3'
QSCN6	5'-GGCTGACCTGGAATCTGCACT-3'	5'-CATTGTGGCAGGCAGAACAAAGTTC-3'
EDIL3	5'-CTGTGAGTGCCAGGCGAATTTA-3'	5'-GATTCATACCCAGAGGCTCAGAACA-3'
MXRA8	5'-GTACACCTGCAACCTGCACCAT-3'	5'-GGGACGATGACATTGATGACGTTGT-3'
PRRT3	5'-GCTGACAGTCACAGGAACCTCTGA-3'	5'-GCCTCTGCAAGTGTTCCCTCAA-3'
LRP1	5'-CAATGGCCTGACGCTGGACTAT-3'	5'-CGGTGTCACACTTCCACCAGA-3'
ISLR	5'-GCTCGCTGCAACTCAACCACAA-3'	5'-CTCAGCACTGCCAGCTCATT-3'
COL6A1	5'-GCAGTACAGCCACAGCCAGAT-3'	5'-GTCAAAGTTGTGGCTGCCAC-3'
TIMP1	5'-GACCTCGTCATCAGGGCCAA-3'	5'-GCAAGGTGACGGGACTGGAA-3'
LAMP1	5'-CACGTTACAGCGTCCAGCTCAT-3'	5'-CCTTGTAGGAAAACCGGCTAGAAC-3'
SERPINH1	5'-CTGCTGCGCTCACTCAGCAA-3'	5'-CGTGATGGGGCATGAGGATGAT-3'
COL1A1	5'-CACCTCAAGAGAAGGCTCACGAT-3'	5'-CCACGCTGTTCTTGCACTGGTA-3'
GAPDH	5'-ACCACAGTCCATGCCATCAC-3'	5'-TCCACCACCCTGTTGCTGTA-3'

The RNA sequences used are as follows: siEF1 (sense 5'-GGCAGCAGAACCCUUCUUAdCdG-3', antisense 5'-UAAGAAGGGUUCUGCUGCCdCdG-3'). SJES-5 cells were plated on a 6-well plate and propagated in RPMI-1640 medium supplemented with 10% FBS. Twenty-four hours later, for transfection, 1 μ l of 10 pmol siRNA was diluted with 99 μ l

of Opti-MEM (Invitrogen), and 2 μ l of siFECTOR reagent (B-Bridge International, Mountain View, CA, USA) was diluted with 98 μ l of Opti-MEM. Both solutions were mixed gently and incubated at room temperature for 5 min. The mixture was diluted with 800 μ l of Opti-MEM, and left at room temperature for 15 min. Next, 1 ml of RNA/liposome

Table III. Genes isolated by the retrovirus-mediated signal sequence trap method (SST-REX).

Isolated gene	Accession number ^a	Frequency ^b
Granulin (GRN)	NM_002087	22
Alzheimer disease amyloid β A4 precursor protein	NM_201414	16
Procollagen-proline, 2-oxoglutarate 4-dioxygenase	NM_000918	14
NODAL modulator 2 (NOMO2)	NM_173614	12
NODAL modulator 1 (NOMO1)	NM_014287	12
NODAL modulator 3 (NOMO3)	NM_001004067	11
Golgi apparatus protein 1 (GLG1)	NM_012201	10
Podocalyxin-like (PODXL)	NM_001018111	6
Lysosomal-associated membrane protein 2 (LAMP2)	NM_013995	6
Insulin-like growth factor binding protein 3 (IGFBP3)	NM_000598	6
Basigin	NM_198589	6
Dystroglycan 1	NM_004393	6
DKFZP56400823 protein	NM_015393	5
Ephrin-A5	NM_001962	4
SPARC	NM_003118	4
CD97	NM_001025160	4
Calreticulin	NM_004343	4
Insulin-like growth factor binding protein 4 (IGFBP4)	NM_001552	4
Poliovirus receptor	NM_006505	3
Syndecan 2	NM_002998	3
Seizure-related 6 homolog like 2	NM_201575	3
CD276	NM_025240	3
TMED7	NM_181836	3
Ribophorin II	NM_002951	3
Niemann-Pick disease, type C1	NM_000271	3
TMEM165	NM_018475	3
MHC class I antigen	NM_005514	3
Colony stimulating factor 2	NM_000758	3
NGFR	NM_002507	2
Ribophorin I	NM_002950	2
Proline-rich transmembrane protein 3	NM_207351	2
Custerin	NM_203339	2
Prosaposin	NM_002778	2
Leucine rich repeat neuronal 6A (LRRN6A)	NM_032808	2
Lysosomal-associated membrane protein 1 (LAMP1)	NM_005561	2
Quiescin Q6	NM_001004128	2
Neuroplastin	NM_017455	2
Reticulocalbin 1	NM_002901	2
Hemicentin 1	NM_031935	2
Matrix metalloproteinase 14 (MMP14)	NM_004995	2
Collagen, type VI, α 1	NM_001848	2
MHC class I polypeptide-related sequence A	NM_000247	2
Low density lipoprotein-related protein 1 (LRP1)	NM_002332	2
TMEM123	NM_052932	2
Collagen, type XV, α 1	NM_001855	2
Protein kinase C substrate 80K-H	NM_002743	2
EGF-like module containing, mucin-like, hormone receptor-like 2	NM_152920	2
Collagen, type I, α 2	NM_000089	2
Lectin, galactoside-binding, soluble, 3 binding protein	NM_005567	2
Collagen, type VII, α 1	NM_000094	2

Table III. Continued.

Isolated gene	Accession number ^a	Frequency ^b
Protein tyrosine phosphatase, receptor type, F	NM_130440	1
Connective tissue growth factor	NM_001901	1
Protein disulfide isomerase family A, member 4	NM_004911	1
Immunoglobulin superfamily containing leucine-rich repeat (ISLR)	NM_005545	1
Collagen, type I, $\alpha 1$	NM_000088	1
Procollagen C-endopeptidase enhancer (PCOLCE)	NM_002593	1
Chromosome 1 open reading frame 56	NM_017860	1
TIMP metalloproteinase inhibitor 1 (TIMP1)	NM_003254	1
Insulin-like growth factor binding protein 5 (IGFBP5)	NM_000599	1
Solute carrier family 24 member 6 (SLC24A6)	NM_024959	1
Neural cell adhesion molecule 2 (NCAM2)	NM_004540	1
Collagen, type V, $\alpha 1$	NM_000093	1
CD248	NM_020404	1
Fc fragment of IgG, receptor, transporter, α	NM_004107	1
Nucleobindin 1	NM_006184	1
delta/notch-like EGF-related receptor (DNER)	NM_139072	1
Limbic system-associated membrane protein (LSAMP)	NM_002338	1
Lysyl oxidase (LOX)	NM_002317	1
Endothelial cell-specific molecule 2 (ECSM2)	NM_001077693	1
Isolate Tor36 (ZE657) mitochondrion	AY738975	1
Lectin, mannose-binding, 1	NM_005570	1
CD99 molecule-like 2	NM_031462	1
EGF-like repeats and discoidin I-like domains 3	NM_005711	1
SIL1 homolog, endoplasmic reticulum chaperone	NM_022464	1
ADAM with thrombospondin type 1 motif, 4 (ADAMTS4)	NM_005099	1
Matrix-remodelling associated 8 (MXRA8)	NM_032348	1
Protein C receptor, endothelial	NM_006404	1
Tissue factor pathway inhibitor	NM_001032281	1
Serpin peptidase inhibitor, clade H member 1 (SERPINH1)	NM_001235	1
Protocadherin γ subfamily A.6	NM_032086	1

^aAccession number in GenBank protein database. ^bNumber of the clones isolated by SST-REX.

complex was added to 1 ml of OPTI-MEM supplemented with 20% FBS. Then, the culture medium of the SJES-5 cells was replaced with the 2 ml of the RNA/liposome-containing medium prepared. Twenty-four hours after transfection, culture medium was replaced with the 2 ml of Opti-MEM with 10% FBS, and grown for another 48 h. The cells were harvested and then total RNA was extracted for RT-PCR analysis. The primers used for RT-PCR are as follows: EWS-FLII-S, 5'-GGGTATGGCACTGGTGCTTATGAT-3'; EWS-FLII-AS, 5'-GGCTCCAAAGAAGCTGGAGGAA-3'; EWS-S, 5'-GCCAGCCCACTCAAGGATAT-3'; EWS-AS, 5'-CCCCTGTGCTAGATTGAGGTTGA-3'; FLII-S, 5'-GCCAACGCCAGCTGTATCA-3'; FLII-AS, 5'-GTGTGAAGGCACGTGGGTGTT-3'.

IP-Western analysis. IP-Western blot analysis was performed as previously described (39) with some modifications. Briefly, cells were lysed in RIPA buffer [50 mM Tris-HCl

(pH 7.4), 150 mM NaCl, 1% NP40, 0.5% deoxycholate, 0.1% SDS]. Cell lysates were immunoprecipitated with the rabbit polyclonal anti-ADAMTS4 antibody. SDS-polyacrylamide gel electrophoresis was performed under reducing conditions using 5-20% gradient gel (Wako Pure Chemical Industries, Osaka, Japan). After transfer to a nitrocellulose membrane, the blot was probed with the rabbit polyclonal anti-ADAMTS4 antibody and then with the HRP-conjugated goat anti-rabbit IgG secondary antibody. ADAMTS4 protein was detected with enhanced chemiluminescence (ECL) Western blotting detection reagents (Santa Cruz Biotechnology).

Immunohistochemical staining. Specimens were retrieved from the patients during surgical resection. Archival tumor blocks were fixed with 10% formaldehyde/phosphate-buffered saline (PBS), and embedded in paraffin. The paraffin-embedded tissues, measuring 4 μ m in thickness, were placed on glass slides (Matsunami Glass, Osaka, Japan) and deparaf-

Table IV. Comparison of the gene expression levels between human mesenchymal stem cells (hMSCs) and Ewing's sarcoma (EWS) cells.

A.	hMSC		EWS
DKFZP56400823	-		+
ADAMTS4	-		+
DNER	-		+
NGFR	-		+
LRRN6A	-		+
ECSM2	-		+
LGALS3BP	-		+
PTPRF	-		+
FCGRT	-		+
B.	hMSC		EWS
LAMP2	+	<	++
RCN1	+	<	+
MMP14	+	<	+
SDC2	+	<	+
DAG1	+	<	+
EPCR	+	<	+
CD97	+	<	+
CD99L2	+	<	+
IGFBP5	+	<	+
CLU	+	<	+
LSAMP	+	<	+
NPTN	+	<	+
EFNA5	+	<	+
PODXL	+	<	+
TMEM123	+	<	+
C.	hMSC		EWS
PCOLCE	+		+
SEZ6L2	+		+
IGFBP4	+		+
IGFBP3	+		+
LOX	+	>	+
CTGF	+	>	+
SPARC	+	>	+
QSCN6	+	>	+
EDIL3	+		+
MXRA8	+		+
PRRT3	+		+
LRP1	+		+
ISLR	+		+
COL6A1	+	>	+
TIMP1	++	>	+
LAMP1	+		+
SERPINH1	+		+
COL1A1	+		+

++, strongly positive; +, moderately positive; -, negative; > or <, >2-fold difference in the expression level.

finished in xylene for hematoxylin and eosin (H&E) and immunohistochemical staining. Antigen retrieval was performed with citrate buffer (pH 6.0) at 97°C for 45 min. After cooling for 60 min and washing in PBS, the rabbit anti-ADAMTS4 antibody (Santa Cruz Biotechnology) diluted 1:50 in antibody diluent buffer (Dako) was reacted. The slides were then washed and incubated with the HRP-conjugated anti-rabbit IgG antibody. The 3-3' diaminobenzidine tetrahydrochloride (DAB) was used for coloration. Hematoxylin was used as the final nuclear counterstaining.

Immunofluorescence staining. The expression of ADAMTS4 protein was analyzed by immunofluorescence. Cells were fixed for 30 min in 4% paraformaldehyde/PBS, and permeabilized for 30 min in 0.1% Triton X/PBS. Fixed cells were rehydrated with Tris-buffered saline, and then incubated with the rabbit polyclonal anti-ADAMTS4 antibody. Immunofluorescence staining was done with the Alexa488-conjugated anti-rabbit IgG antibody. Nucleus was detected with bis-benzimide (Hoechst-33342, Sigma-Aldrich) staining.

ELISA. To evaluate the expression level of secreted ADAMTS4 protein, supernatants of the EWS cell lines and the patient sera were subjected to ELISA. The 96-well plates were coated with the monoclonal anti-human ADAMTS4 antibody at 4°C overnight. After 3 washes with washing buffer (0.05% Tween-20/PBS), the plates were treated with 10% FBS in PBS for 1 h at room temperature. The recombinant human ADAMTS4 (amino acids 213-685) diluted with 10% FBS in PBS, as standard proteins, and the samples were added to each well, and incubated at room temperature for 2 h. After 5 washes with washing buffer, the Avidin-HRP and the biotinylated anti-human ADAMTS4 detection antibody were added to each well, and incubated for 1 h at room temperature. After 7 washes with washing buffer, 100 µl of tetramethylbenzidine buffer as a substrate was added to each well and incubated for 30 min at room temperature in the dark. Color development was stopped by addition of 100 µl of stop solution (1 N H₃PO₄). Optic density of each sample was measured at 450 nm.

Results

Analysis of isolated cDNA clones. In SST-REX screening, we isolated 322 factor-independent Ba/F3 clones (Table III). Sequencing analyses revealed that integrations derived from 256 clones harbored the signal sequence. Among them, 80 different secreted and type I membrane proteins were identified. We used the database of RefEX, PubMed, ONCOMINE and SMART for the analysis, and 42 proteins that might be related to tumor/cancer onset and progression were selected.

Recent studies have suggested that the origin of EWS is derived from hMSC (40,41). To examine the expression levels of these 42 molecules in EWS in comparison with hMSC, we performed RT-PCR analysis (Table IV). They were classified into 3 groups by mRNA expression profiles; the first group with high expression levels only in EWS (Table IVA), the second group with higher expression levels in EWS than in hMSC (Table IVB), and the third group with similar or lower expression levels in EWS compared with

Table V. Gene expression levels in murine tissues by RT-PCR analysis.

	Brain	Heart	Lung	Liver	Kidney	Spl	Stm	S. int	L. int	Mus	Tes	Thy	BM	OC
DKFZP56400823	+	+	+	-	+	+	+	+	+	+	+	+	+	+
ADAMTS4	++	+	-	+	-	-	-	-	-	+	-	-	+	+
DNER	++	-	-	-	-	-	-	-	-	-	+	-	-	+
NGFR	+	+	-	+	+	-	-	-	-	-	-	-	-	-
LRRN6A	++	-	-	-	-	+	-	+	+	+	+	+	+	+
ECSM2	+	+	+	+	+	-	+	-	-	+	+	+	+	+
LGALS3BP	+	+	+	+	+	+	++	++	+	+	++	++	+	+
PTPRF	+	+	+	+	+	-	+	+	+	+	+	+	-	-
FCGRT	+	+	+	+	+	+	+	+	+	+	+	+	+	+
LAMP2	+	++	+	+	++	++	+	+	+	+	+	+	+	+
RCN1	+	+	+	+	+	-	+	-	-	-	+	+	+	+
MMP14	+	+	+	+	+	-	+	-	-	+	+	+	+	+
SDC2	+	+	+	+	+	-	+	+	-	+	+	+	+	+
DAG1	+	+	+	+	+	+	+	+	+	+	+	+	+	+
EPCR	+	+	+	+	+	+	+	-	-	+	+	+	+	++
CD97	+	+	+	+	+	+	+	+	+	+	+	+	+	+
CD99L2	+	+	+	+	+	-	-	-	-	+	+	+	+	+
IGFBP5	+	+	+	+	+	+	+	+	+	+	+	+	+	+
CLU	+	+	+	+	+	+	+	+	-	+	+	+	+	+
LSAMP	++	+	-	+	+	-	+	-	-	-	+	+	+	+
NPTN	+	+	+	+	+	-	+	+	+	+	+	+	+	+
EFNA5	+	+	+	+	+	-	+	+	+	-	+	+	-	-
PODXL	+	+	+	+	+	-	-	-	-	+	-	-	+	-
TMEM123	-	+	-	+	+	-	-	-	-	+	-	-	-	-

Spl, spleen; stm, stomach; s. int, small intestine; l. int, large intestine; mus, muscle; tes, testis; thy, thymus; BM, bone marrow; OC, osteoclast; ++, strongly positive; +, modelately positive; -, negative.

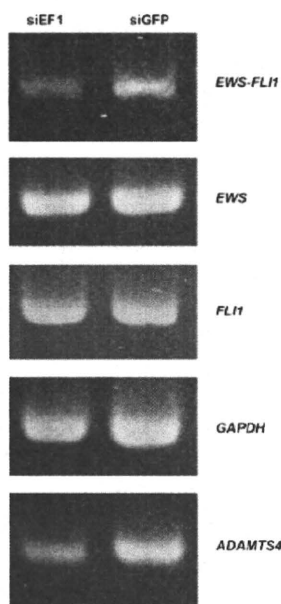


Figure 1. Effects of *EWS-FLI1* suppression on *ADAMTS4* expression. RNA from Ewing's sarcoma cells treated with either siEF1 or siGFP were subjected to RT-PCR experiment. *ADAMTS4* mRNA expression was down-regulated after treatment with *EWS-FLI1*-specific siRNA. *GAPDH* (glyceraldehyde 3-phosphate dehydrogenase) was used as an internal control.

hMSC (Table IVC). We picked up 24 molecules from the first and second groups, and examined the expression patterns in murine organs. As shown in Table V, most molecules did not exhibit interesting tissue distribution patterns. However, some of the molecules attracted us by their expression profiles or their novelty as a gene. We focused on 5 molecules: *ADAMTS4*, *DNER* (*delta/notch-like EGF-related receptor*), *NGFR* (*nerve growth factor receptor*), *LRRN6A* (*leucine rich repeat neuronal 6A*) and *ECSM2* (*endothelial cell-specific molecule 2*). We then examined expression levels of these 5 molecules in various solid tumor and hematopoietic cell lines by RT-PCR. As shown in Table VI, expression levels of *ADAMTS4* were higher in EWS, glioblastoma and neuroblastoma in comparison with other cell lines. These results suggested that *ADAMTS4* is one of the first candidate molecules as a marker for EWS among the SST clones.

ADAMTS4 expression is upregulated by *EWS-FLI1*. Previous studies indicated the expression of the fusion gene, *EWS-FLI1*, was suppressed by using antisense oligonucleotide or siRNA. To decrease the expression level of *EWS-FLI1* in the EWS cell line, we made an siRNA duplex specifically directed against the fusion junction of *EWS-FLI1* transcript. *EWS-FLI1*-specific siRNA (siEF1) was used for SJES-5 cell line. As a control, siGFP was also used. Transfection of siEF1,

Table VI. Gene expression levels of *ADAMTS4*, *DNER*, *NGFR*, *LRRN6A* and *ECSM2* in human cancer cell lines by RT-PCR analysis.

	ADAMTS4	DNER	NGFR	LRRN6A	ECSM2
AsPC-1	-	-	+	-	-
BxPC-3	-	+	-	-	-
Capan-1	-	-	-	-	-
U87MG	+	+	-	-	-
U251	+	++	-	-	-
T98G	-	+	-	-	-
HGC-27	+	-	+	+	-
MKN45	-	+	-	++	-
GCIY	+	+	-	+	-
KATOIII	-	-	-	-	-
MG63	-	+	+	+	+
HOS	+	+	+	+	+
KHOS/NP	-	+	+	+	+
SaOS2	-	+	+	-	-
U2OS	-	+	+	+	-
KPNSI-FA	+	++	+	+	-
LAN-1	+	+	+	+	-
NB69	++	-	+	+	+
H460	+	++	-	+	-
PLC/PRF/5	-	+	+	+	+
HuCC1	-	++	-	+	+
SW48	-	+	+	-	+
RMS	++	++	+	++	+
SJRH-30	++	+	+	+	+
SJES-2, 3, 5, 6, 7, 8	++	++	+	++	++
MOLM13	-	-	-	-	-
ML1	-	-	-	-	-
U937	-	-	-	-	+
Jurkat	-	-	-	-	+
PEER	-	-	-	-	+
CEM	++	-	-	-	+
HPB-ALL	-	-	-	-	-
NALM24	+	+	-	-	+
NALM16	-	+	+	-	-
IM9	-	-	+	-	+

++: strongly positive; +, moderately positive; -, negative.

but not siGFP, led to significant decrease of the expression level of the *EWS-FLI1* fusion transcript (Fig. 1). In agreement with the specificity of siEF1 against the *EWS-FLI1* fusion gene, the expression level of *EWS* or *FLI1* was not affected. Interestingly, suppression of *EWS-FLI1* expression resulted in decreased expression of *ADAMTS4* transcript. These results suggested that *ADAMTS4* expression was upregulated by *EWS-FLI1*.

Immunohistochemical analysis on ADAMTS4 protein expression. In order to confirm the expression of *ADAMTS4*

in EWS at the protein level, we stained 25 tissue samples derived from EWS patients with the anti-*ADAMTS4* antibody together with the H&E staining. *ADAMTS4* protein was detected in 10 EWS samples, but not in 15 samples where tumors disappeared by chemotherapy (Fig. 2 and data not shown).

Next, to examine the subcellular localization of *ADAMTS4*, we stained EWS cell lines with the anti-*ADAMTS4* antibody. Immunofluorescence microscopy revealed that *ADAMTS4* protein was expressed mainly in the cytoplasm of EWS cell lines (Fig. 3C and D) and of the

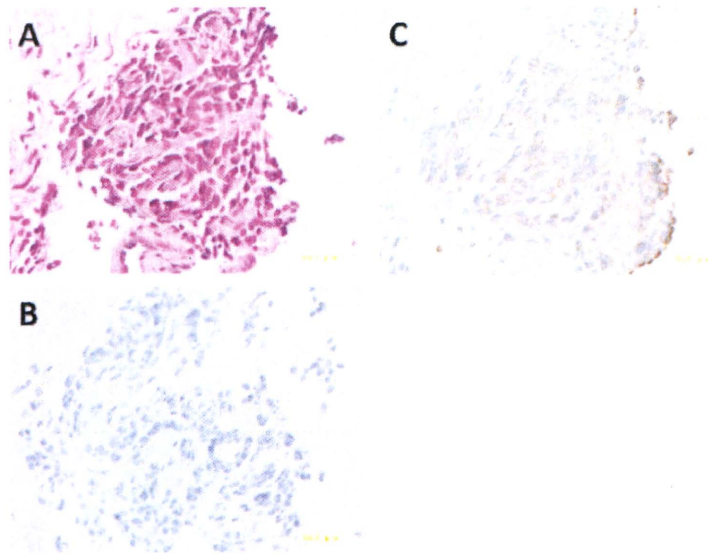


Figure 2. Immunohistochemical analysis of ADAMTS4 protein in the tissue section of the patient with Ewing's sarcoma. (A) Hematoxylin and eosin staining, (B) rabbit IgG, (C) anti-ADAMTS4 antibody.

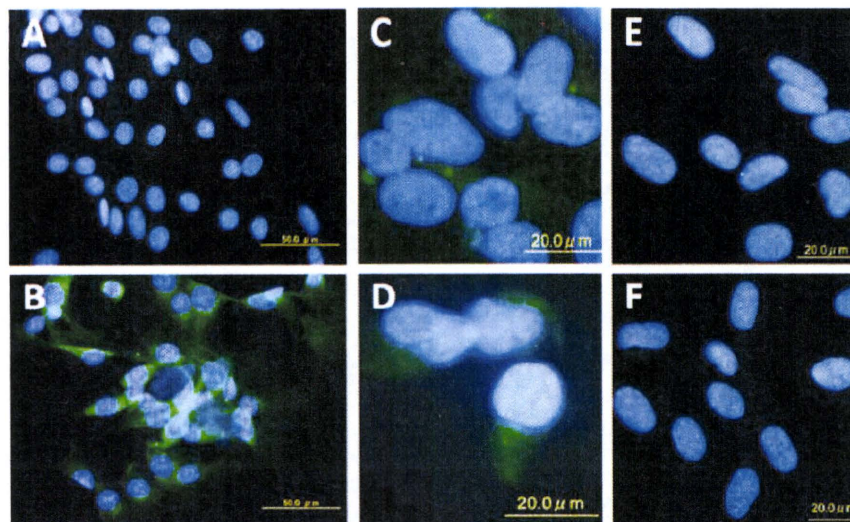


Figure 3. Immunofluorescence staining of ADAMTS4 protein in Ewing's sarcoma cell lines (SJES-2 and SJES-5), osteosarcoma cell lines (MG63 and SaOS2) and NIH3T3 cells expressing ADAMTS4. (A) NIH3T3, (B) ADAMTS4/NIH3T3, (C) SJES-5, (D) SJES-2, (E) MG63, (F) SaOS2.

NIH3T3 cells expressing human ADAMTS4 (Fig. 3B). In contrast, ADAMTS4 was not detected in osteosarcoma cell lines MG63 and SaOS2 (Fig. 3E and F), which did not express *ADAMTS4* at the transcription level (Table VI).

ADAMTS4 is secreted from EWS cells. We next asked whether ADAMTS4 was secreted from EWS cells. First the immunoprecipitates of the cell lysates of EWS cell lines and positive and negative control cells with the anti-ADAMTS4 antibody were electrophoresed, blotted and probed with the same antibody. ADAMTS4 was detected in EWS cells and the positive control cells as double bands of ~100 kDa (Fig. 4A). We next performed the same experiments using 2 ml each of the supernatants of these cells. Notably, significant levels

of expression of ADAMTS4 protein were observed in the supernatants of EWS cells and ADAMTS4/NIH3T3 cells (Fig. 4B). These results suggested that ADAMTS4 was secreted.

Comparative study of ADAMTS4 gene expression in 5 types of sarcomas. We showed that *ADAMTS4* transcripts were expressed in EWS, osteosarcoma and rhabdomyosarcoma cell lines (Table VI). However, whether *ADAMTS4* transcripts are expressed in tumor tissue samples remained unknown. Therefore, we tested if *ADAMTS4* was expressed in soft tissue sarcomas and bone tumors including osteosarcoma, EWS, chondrosarcoma, synovial sarcoma and rhabdomyosarcoma (Fig. 5). Benign tumors including lipoma, desmoid

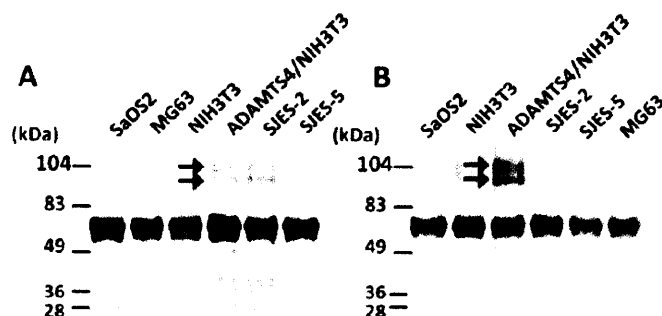


Figure 4. Detection of secreted ADAMTS4 protein. The cell lysates or culture supernatants were immunoprecipitated with the anti-ADAMTS4 antibody, resolved by SDS-PAGE, blotted and probed with the anti-ADAMTS4 antibody. Molecular size markers are shown on the left. Arrows indicate the ADAMTS4 proteins. (A), cell lysates; (B), supernatants.

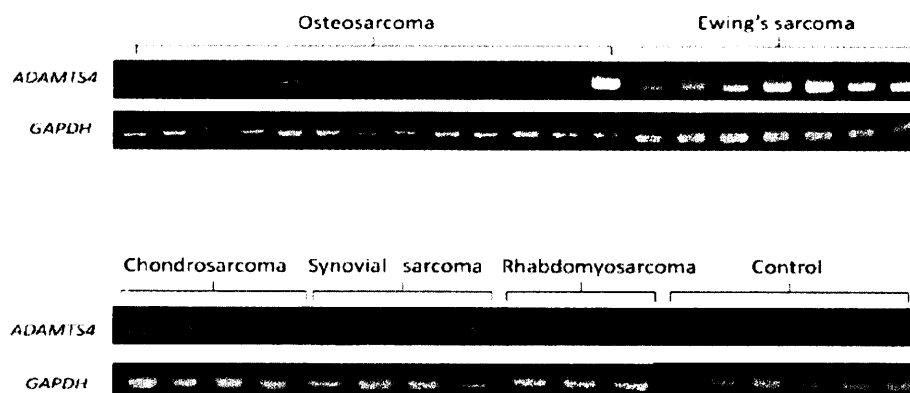


Figure 5. RT-PCR analysis of *ADAMTS4* expression in the patient samples. *GAPDH* expression was used as an internal control.

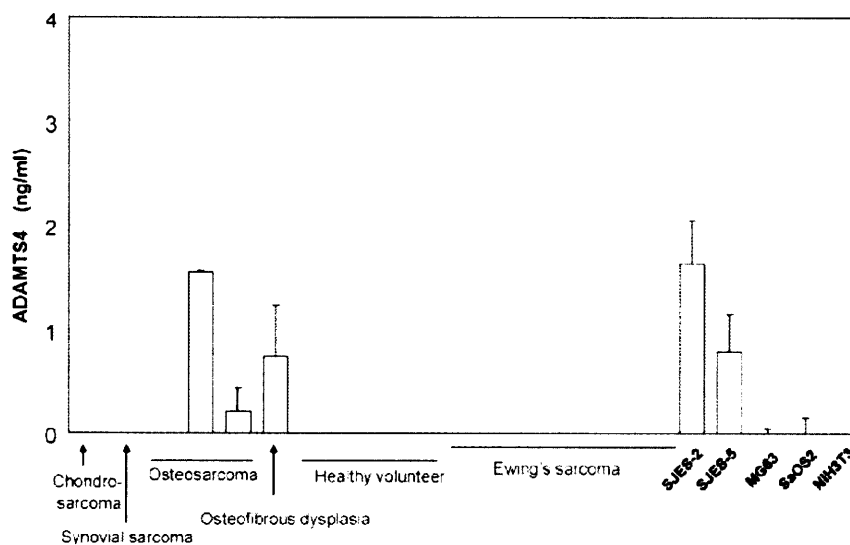


Figure 6. ELISA of ADAMTS4 protein in the patient sera and the supernatants of the cell lines. The error bars represent 1 standard deviation.

and Schwannoma were also examined as controls. In all 7 EWS samples, *ADAMTS4* transcripts were highly expressed. Three out of 4 samples of chondrosarcoma moderately expressed *ADAMTS4*. This result was predictable, since

ADAMTS4 is expressed in normal cartilage cells. Also, 2 out of 13 samples of osteosarcoma and 1 out of 4 samples of synovial sarcoma expressed *ADAMTS4*. *ADAMTS4* transcripts were not detected in the 3 samples of rhabdomyo-